Combustion and emissions characterization of terpenes with a view to their biological production in cyanobacteria

Paul Hellier [a,*], Lamya Al-Haj [b], Midhat Talibi [a], Saul Purton [b], Nicos Ladommatos [a]

[a] Department of Mechanical Engineering, University College London, Torrington Place, London WC1E 7JE, United Kingdom
[b] Institute of Structural and Molecular Biology, University College London, London WC1E 6BT, United Kingdom

HIGHLIGHTS

- Twelve terpenes were tested as pure fuels in a direct injection diesel engine.
- The terpenes are potential products of a genetically engineered cyanobacteria.
- Molecular structure of the terpenes impacted significantly on ignition quality.
- Four terpenes were tested as diesel and gasoline extenders up to 60% terpene.
- Terpene toxicity to the suggested producing cyanobacteria was also assessed.

ARTICLE INFO

ABSTRACT

In developing future fuels there is an opportunity to make use of advances in many fields of science and engineering to ensure that such fuels are sustainable in both production and utilization. One such advance is the use of synthetic biology to re-engineer photosynthetic micro-organisms such that they are able to produce novel hydrocarbons directly from CO_2. Terpenes are a class of hydrocarbons that can be produced biologically and have potential as liquid transport fuels. This paper presents experimental studies on a compression ignition engine and spark ignition engine in which the combustion and emissions of 12 different terpenes that could potentially be produced by cyanobacteria were assessed as single components and blends with fossil diesel and fossil gasoline. The 12 terpenes were chosen to explore how small changes to the molecular structure of geraniol (a terpene most easily produced by cyanobacteria) impact on combustion and emissions. Furthermore, the toxicity of some of the best performing terpenes were assessed using the model cyanobacterium *Synechocystis* sp. PCC6803 (hereafter, *Synechocystis*) as a prelude to a metabolic engineering programme. The compression ignition engine tests were carried out at constant injection timing and constant ignition timing, and the spark ignition engine tests were conducted at a constant spark timing and a constant lambda value of 1. Of the terpenes tested in the compression ignition engine, geranial and farnesene were found to be the best performing single component fuels in terms of combustion and emissions. In blends with fossil diesel, the presence of geranial or farnesene did not have a significant effect on combustion phasing up to a terpene content of 20% (wt/wt), though levels of NOx and CO did increase. In the spark ignition engine experiments of terpene and fossil gasoline blends, citronellene and linalool were found to be soluble in fossil gasoline and combusted in a steady manner up to a terpene content of 45% and 65% (wt/wt) respectively. Of those terpenes with the most potential as either diesel or gasoline fuels, geraniol and geranial were found to be the most toxic to *Synechocystis*, with farnesene and linalool less toxic and citronellene having no detrimental effect. Addition of *n*-dodecane to the cultures was found to ameliorate the toxic effects of all five terpenes.

© 2013 Elsevier Ltd. All rights reserved.

1. Introduction

The advent of genetically engineered micro-organisms is an exciting opportunity to explore novel and sustainable methods of bio-fuel production [1,2]. While the introduction of novel biosynthesis pathways into micro-organisms is a field still very much in its infancy, un-modified micro-organisms have already seen considerable utilization in industrial applications [3]. Yeasts have been utilized for several decades in the large scale production of bio-ethanol via fermentation of sugars [4]. More recently, the use of algal lipids for the production of bio-diesel via transesterification of fatty

* Corresponding author. Tel.: +44 20 7679 7620; fax: +44 20 7388 0180.
E-mail addresses: p.hellier@ucl.ac.uk, hellier.pr@gmail.com (P. Hellier).

Nomenclature

NOx	nitrogen oxides	SOC	start of combustion
CO_2	carbon dioxide	SOC2	start of 2nd phase of combustion and point between SOC and the time of peak heat release rate at which $d(\tan^{-1}(dHRR/dCAD)$ is at a minimum and dHRR is positive.
IQT	ignition quality testing		
CFR	cooperative fuels research		
DCN	derived cetane number		
CO	carbon monoxide	IMEP	indicated mean effective pressure
THC	total hydrocarbons	FAME	fatty acid methyl ester
CAD	crank angle degree	RON	research octane number
PID	proportional integral derivative	*E. coli*	*Escherichia coli*
DAQ	data acquisition	DNC	did not combust
O_2	oxygen	Dp	Mean particle diameter
SOI	start of injection		
BTDC	before top-dead-centre		
TDC	top-dead-centre		

acids with an alcohol is attracting significant interest [5–8], with favorable comparisons to other lipid sources [9,10]. However, while the feedstock is renewable, the production of algal bio-diesel via lipid extraction and transesterification does not yet represent a low-carbon route to replace fossil fuels. It is also, at present, generally considered economically non-viable without either government subsidy or a decline in global oil resources and a concurrent escalation in the price of crude fossil oil [11–13]. This economic non-viability can in part be attributed to the large energy cost associated with the harvesting and drying of algal cells that grow in aqueous media at densities typically less than 10 g/L [14] and is currently considered to be a major limitation of biochemical production from photosynthetic organisms [15]. Therefore, the possibility of engineering a microalga in such a way so as to negate this prohibitive energy cost is highly attractive.

There has been considerable progress in recent years in the use of synthetic biology approaches to re-engineer metabolic pathways in heterotrophic bacteria such as *Escherichia coli* to produce a range of novel hydrocarbons that could be used as fungible fuel molecules [1]. These candidate biofuels include alkanes, alkenes,

alcohols and terpenoids. Furthermore, efflux systems engineered into the bacteria should allow for the excretion of the product into the medium, thereby avoiding toxic build-up in the cell and circumventing the need for cell harvesting and extraction [16]. If similar metabolic engineering approaches can be applied to photosynthetic micro-organisms such as eukaryotic microalga or cyanobacteria, then an efficient biological system for direct light-driven conversion of CO_2 into advanced biofuels could be envisaged. Of the two groups of organisms, cyanobacteria are the more attractive as a chassis for such metabolic engineering, not least because species can be found that are fast-growing and tolerant to a range of abiotic stresses (high temperature, high light, high salt, etc.), and their simpler genetics and physiology make them easier to engineer [17]. Indeed, promising initial work has been reported in which the model species, *Synechocystis* or other genetically tractable species have been engineered to produce a range of bio-industrial compounds including biofuels [18].

A particularly attractive target for biofuel engineering in cyanobacteria is the terpenoid (or isoprenoid) pathway, which is responsible for the biosynthesis of a diverse range of compounds using
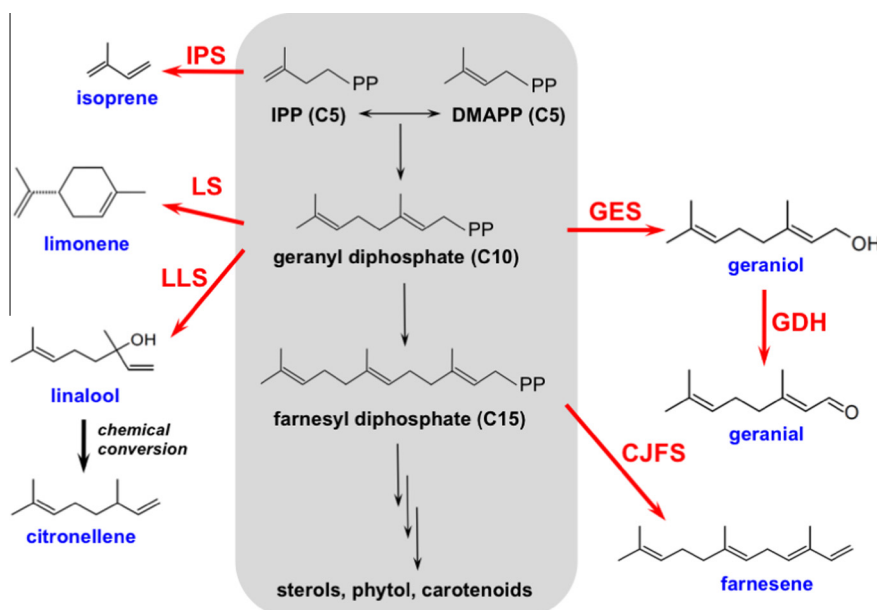

Fig. 1. The isoprenoid pathway (highlighted in gray) and examples of possible pathways (red arrows) that could be introduced to produce novel hydrocarbons (blue). IPS: isoprene synthase; LS: limonene synthase; LLS: linalool synthase; GES: geraniol synthase; GDH: geraniol dehydrogenase; CJFS: (*E*)-b-farnesene synthase.

five-carbon isoprene units as building blocks [19]. Fig. 1 gives an overview of the basic pathway and highlights how the introduction of additional enzymes could create novel C5, C10 or C15 terpene products. In many cases, only a single enzyme such as isoprene synthase or geraniol synthase is required, although additional enzymes could be employed to further modify the product. To-date, there are only two reports of such engineering in cyanobacteria with the products being isoprene [20], and the sesquiterpene, -caryophyllene [21]. Whilst these pathways look attractive, an important consideration is the toxicity of these hydrophobic products to the cyanobacterial host, and how this can be mitigated by lowering the steady-state concentration of product: for example, using efflux pumps within the cell membrane or an organic solvent phase in the culture vessel [16,22].

Whilst there has been a great deal of work investigating the potential of fatty acid esters to fuel compression ignntion engines, terpenes and especially monoprenoids have to date received significantly less attention. Tracy et al. [23] hydrogenated the monoterpenes myrcene and limonene and blended the products with fossil diesel at 5–10%. All of the blends met the minimum standards of ASTM D975, though in the case of the hydrogenated products of myrcene (comprising 84.5% 2,6-dimethyloctane), the viscosity of the blends was higher than that for the fossil diesel. Peralta-Yahaha et al. [24] produced the monocyclic sesquiterpene bisabolene by metabolic engineering of *E. coli* and also the yeast *Saccharomyces cerevisiae*. The sesquiterpene was hydrogenated to form bisabolene, and was determined by ignition quality testing (IQT) to possess a cetane number of between 41.9 and 52.6. Anand et al. [25] investigated the combustion and emissions production of a turpentine oil (consisting of at least 40% pinene) in a direct injection diesel engine and found the turpentine oil to have a cetane number of 38. At a fixed injection timing of 23 BTDC they found that emissions of NOx, CO and THC all decreased up to a blend level of 50% turpentine oil in diesel, concurrent with the movement of peak heat release earlier into the compression stroke. Combustion of pure turpentine oil was somewhat less steady than the fossil diesel, as indicated by greater variation in the peak cylinder pressure.

This paper presents the results of an investigation into the potential of cyanobacterial produced terpene bio-fuels, specifically geraniol and several other terpenes that represent a change to the molecular structure of geraniol. The work consists of experiments assessing terpene combustion characteristics and emissions production in compression ignition and spark ignition engines as single components and blends with fossil fuels, and terpene toxicity to the producing cyanobacterium.

2. Experimental methods

2.1. Engine combustion and emissions experiments

2.1.1. Apparatus

All combustion experiments in which the terpenes were tested as single component fuels, or blended with fossil diesel, were conducted in a single cylinder direct injection compression ignition engine specially designed for combustion research. Several of the fuels tested were available in only small quantities at the high assay required, or had physical properties, such as low lubricity, which would have resulted in damage to the fuel pump and common rail components. So, to overcome these issues, a previously designed and manufactured [26] low volume, high injection pressure fuel system was utilized.

Based on the concept first proposed and implemented by Schönborn et al. [27], the system uses the engine common rail system as a hydraulic fluid supply so as to pressurize a small quantity of the sample fuel (100–250 ml) via two free pistons. The redesigned system used for the tests discussed in this paper features a bypass operated by high pressure needle valves that allows fossil diesel fuel from the engine pump circuit to flow at pressure through the test fuel circuit. This allows the fuel system and combustion chamber to be flushed with a reference diesel between every test run. A schematic of the system is given in Fig. 2. The sample fuel was supplied to the engine fuel injector via a 1 μm sintered filter element. The injector nozzle had six holes, each of 154 μm diameter. The sample fuel lines and low volume fuel system were all held at a constant temperature, of up to $63 \pm 4\ ^\circ C$, by several heating elements divided into five zones, each controlled by a separate PID controller on account of the widely differing thermal properties of each zone. Further details of the compression ignition engine and control apparatus are given in Table 1.

Combustion experiments in which the terpenes were blended with gasoline were conducted in a Ricardo E6 single cylinder research spark ignition engine. Fuel and air were mixed in a carburetor approximately 150 mm upstream of the engine intake valves and subsequently ignited by a spark plug (NGK B7HS) within the cylinder. Further details of the E6 spark ignition engine and control apparatus are given in Table 2.

In the case of both the compression and spark ignition engines, the cylinder gas pressure was measured and logged with a PC data acquisition system (National instruments) using a piezoelectric pressure transducer (Kistler 6056AU38 and cooled Kistler 6041A
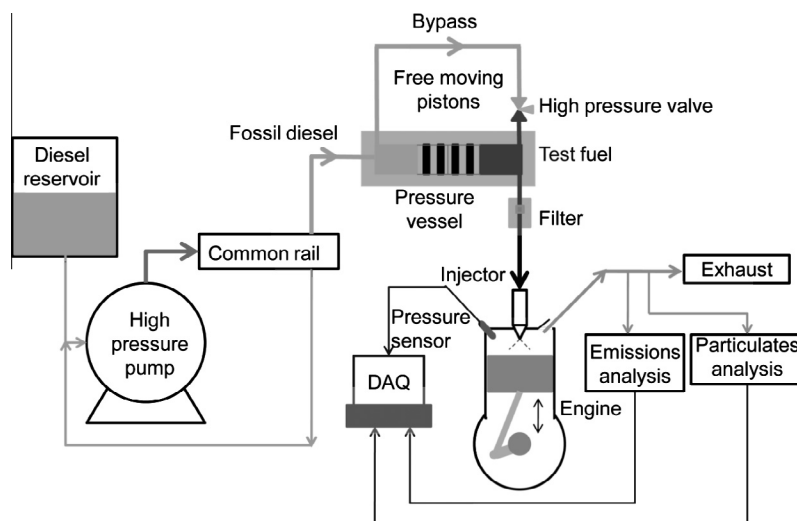

Fig. 2. Schematic showing operation of the low volume fuel system.

Table 1
Compression ignition engine specification.

Engine head model	Ford Duratorq
Engine bottom end model	Ricardo Hydra
Number of cylinders	1
Cylinder bore	86 mm
Crankshaft stroke	86 mm
Swept volume	499.56 cc
Compression ratio	15.8:1
Maximum cylinder pressure	150 bar
Peak motoring pressure at test conditions	36 bar
Piston design	Central ω-bowl in piston
Oil temperature	80 ± 2.5 °C
Water temperature	80 ± 2.5 °C
Fuel injection pump	Single-cam radial-piston pump (BOSCH CP3)
High pressure fuel rail	Solenoid controlled, max. 1600 bar (BOSCH CRS2)
Injectors	6-Hole solenoid controlled (DELPHI DFI 1.3)
Electronic fuel injection system	1 μs resolution (EMTRONIX EC-GEN 500)
Shaft encoder	0.2 CAD resolution

Table 2
Spark ignition engine specification.

Engine model	Ricardo E6
Number of cylinders	1
Cylinder bore	76.2 mm
Crankshaft stroke	55.57 mm
Swept volume	506.8 cc
Compression ratio	10.3:1
Oil temperature	40 ± 2.5 °C
Water temperature	40 ± 2.5 °C
Fuel delivery system	Single barrel, fixed venturi carburetor
Shaft encoder	0.4 CAD resolution

respectively) and charge amplifier (Kistler 5011 and Kistler 5007 respectively). At bottom-dead-centre of every combustion cycle the cylinder pressure was pegged by the data acquisition system. In the case of the diesel engine this was performed using a piezo-resistive pressure transducer (Druck PTX 7517-3257) located in the intake manifold, 160 mm upstream of the inlet valves, and for the gasoline engine a value of atmospheric pressure was used. The compression and spark ignition engines were both naturally aspirated with a geometric compression ratio of 15.8:1 and 10.3:1 respectively. For all the tests, air was supplied to the engines at atmospheric pressure but for some tests with the compression ignition engine the air was heated to a temperature of 133.5 ± 2.4 °C before being supplied to the engine. This elevated temperature was achieved via the use of an inline air heater (Secomak 571), situated approximately 200 mm upstream of the intake manifold, with the 2 kW heater held at constant temperature by a PID temperature controller (CAL 9900). For both engines, various control and experiment temperatures were measured with K-type thermocouples and logged with the same PC data acquisition system utilized in recording in-cylinder pressures. The net apparent heat release rate was derived from the measured in-cylinder pressure during post-processing (MATLAB), as were the global gas temperatures utilizing the ideal gas law and calculated values of the total cylinder volume at a given crank angle degree (assuming the cylinder contents to be a homogenous ideal gas).

For combustion experiments with the compression ignition engine, exhaust gas sampling occurred 180 mm downstream of the exhaust valves to determine concentrations of gaseous species and also particulate size distribution. A gas analyzer system

(Horiba MEXA 9100 HEGR), supplied with sample gas via heated lines, was used to measure the following: NOx concentrations by chemiluminescence (at an accuracy of ±0.1 ppm); CO and CO_2 concentrations with non-dispersive infrared (at an accuracy of ±0.1 ppm and ±0.1% vol/vol respectively); paramagnetic analysis to determine O_2 concentrations (at an accuracy of ±0.01% vol/vol); and levels of un-burnt hydrocarbons were measured with a flame ionization detector (at an accuracy of ±1 ppm). Size and mass distributions of the sub-micron particles in the exhaust gas were determined by a differential mobility spectrometer (Cambustion DMS500). Sampling of exhaust gases for particulate measurements was made via a heated line, with a dilution cyclone located at the connection between the engine exhaust and heated line. Exhaust gases were diluted at this point by 4:1 and were diluted a second time upon entry to the analyzer by 100:1. The sample line and both dilution cyclones were heated to a constant temperature of 75 °C. For experiments utilizing the spark ignition engine emissions were not measured, however the value of lambda was determined using an air-fuel ratio (AFR) sensor (ECM AFRecorder 1200) located 120 mm downstream of the exhaust valve.

2.1.2. Fuel molecules investigated

The C10 compound, geraniol which could potentially be produced in *Synechocystis* using a single enzyme (Fig. 1) and a further 11 others, were tested in the compression ignition engine as single component fuels. The 11 molecules possessed molecular structures, in most cases, not dissimilar to geraniol and were thus chosen as they could potentially either be produced instead of geraniol via additional enzymes added to the pathway (Fig. 1), or post-processed from geraniol by chemical or physical methods. Furthermore, the 11 molecules were chosen to provide an insight as to how the following changes to molecular structure would impact on combustion phasing and emissions production:

(a) *Cis* vs *trans* isomerization of geraniol (geraniol and nerol).
(b) Increasing the degree of saturation while keeping all other aspects of molecular structure constant (geraniol, citronellol and 3,7-dimethyl-1-octanol).
(c) Movement of the OH within a monoprenoid (geraniol and linalool).
(d) Replacement of the OH group of a monoprenoid with other oxygen containing functional groups (geraniol, geranyl acetate, geranial, citral dimethyl acetal and (−)-β-citronellene).
(e) Comparison of an monoprenoid and cyclic compound with identical carbon and oxygen content (geraniol and L-menthol).
(f) Increasing the carbon chain length of sesquiterpenes (farnesene and squalene).

Alongside the 12 single component fuels, a reference fossil diesel with zero FAME content and a reference fossil gasoline with zero alcohol content were also tested. All of the pure component fuels were obtained from a chemical supplier (Sigma Aldrich). The assay and other properties of each fuel are presented in Table 3, while the molecular structure of each is given in Table 4.

2.1.3. Experimental conditions

2.1.3.1. Compression ignition engine experiments. Each of the 12 molecules and reference diesel were initially tested at two experimental conditions: constant fuel injection timing and constant start of ignition timing. At constant injection timing the start of injection (SOI, defined as the time at which the injector actuating signal commences) was held constant at 7.5 CAD BTDC, and the start of combustion for each fuel varied according to the ignition delay of that fuel. For constant ignition timing, the SOI was varied so that the SOC of all fuels always occurred at TDC. SOC was

Table 3
Fuel properties.

	Molecular formula	Assay (%)	T_{boil} (°C)	T_{melt} (°C)	$\Delta vapH°$ (kJ/mol)	Density at 20 °C (kg/m³)	Dynamic viscosity at 19.7 °C (mPa s)	Dynamic viscosity at 59.7 °C (mPa s)
Reference fossil diesel	–	–	269[b]	–	–	834.5[a]	3.42	1.75
Geraniol	$C_{10}H_{18}O$	⩾97	229.9 – 231 [28,29]	−15 [30]	–	880.1 [28]	8.28	2.85
Nerol	$C_{10}H_{18}O$	⩾97	226.2 [28]	–	–	876 [28]	7.19	2.52
Citronellol	$C_{10}H_{20}O$	⩾95	224.9 [29]	–	–	855.1 [31]	11.50	3.30
3,7-Dimethyl-1-octanol	$C_{10}H_{22}O$	⩾98	–	–	66.15 [32]	830.8 [33]	15.33	3.82
Linalool	$C_{10}H_{18}O$	⩾97	198 [34]	–	–	862.4–872 [35,36]	4.47[c][35]	1.84
Geranyl acetate	$C_{12}H_{20}O_2$	⩾98	–	–	–	915 [37]	3.03	1.63
Geranial (citral-A)	$C_{10}H_{16}O$	⩾95	225–227 [38]	–	–	886.8 [38]	2.65	1.48
Citral dimethyl acetal	$C_{12}H_{22}O_2$	⩾90	–	–	–	–	2.41	1.37
(−)-β-Citronellene	$C_{10}H_{18}$	⩾90	158.85 [39]	–	–	760.1 [40]	1.00	0.84
ʟ-menthol	$C_{10}H_{20}O$	⩾99	214.6 [41]	42.5 [42]	–	913.1 [43]	–	6.17
Farnesene (mixture of isomers)	$C_{15}H_{24}$	–	–	–	–	841 [44]	3.29	1.70
Squalene	$C_{30}H_{50}$	⩾98	–	−5.2 to −4.8 [45]	–	857.7 [46]	15.50	5.49

[a] Experimental data obtained according to ASTM D4052 at 15 °C.
[b] Experimental data obtained according to EN ISO 3405.
[c] Data at 25 °C. Values of viscosity were measured at temperatures of 19.7 °C and 59.7 °C using a stand-alone rheometer (Brookfield LVDV – III + U).

Table 4
Fuel structures.

Geraniol

Nerol

Citronellol

3,7-Dimethyl-1-octanol

Linalool

Geranyl acetate

Geranial (citral-A)

Citral dimethyl acetal

(−)-β-Citronellene

ʟ-menthol

Farnesene (mixture of isomers)

Squalene

Fig. 3. Definition of SOC and SOC2 in terms of apparent net heat release rate (HRR), cumulative heat release rate, 1st derivative of heat release rate (dHRR) and d(tan⁻¹(dHRR/dCAD)) where dCAD is the 1st derivative of the crank angle position.

displayed in Fig. 3. SOC2 is defined as the minimum value of d(tan⁻¹(dHRR/dCAD)) between SOC and the time of peak heat release where dHRR is positive, and is indicative of the commencement of the bulk of heat release through detection of a significant change in the gradient of heat release rate.

All single component fuels (including the reference diesel) were first heated in a PID controlled water bath held at 60 °C prior to filling of the low volume fuel system which had been preheated to 63 ± 4 °C and was held at this temperature throughout the subsequent experiment. Inlet air for all experiments was heated to 133.5 ± 2.4 °C. The elevated temperatures of both the fuels and engine inlet were chosen as preliminary experiments revealed that at lower temperatures geraniol combusted in an increasingly unsteady manner, unsuitable as a benchmark for comparison of the combustion properties of the other terpenes.

All tests of single components fuels were conducted at an engine speed of 1200 rpm and at 700 bar fuel injection pressure. The injection duration was adjusted in the case of every fuel so that the engine IMEP was always constant at 4.00 bar for all fuels, with a summary of the engine and test operating conditions given in Table 5.

A further series of experiments was undertaken in which two of the molecules, farnesene and geranial, were blended in varying

defined as the time in CAD (after SOI and before the time of peak heat release rate) at which the minimum value of cumulative heat release occurs.

In Fig. 3, heat release rate (HRR), cumulative heat release rate, the 1st derivative of heat release rate (dHRR) and d(tan⁻¹(dHRR/dCAD)), where dCAD is the 1st derivative of crank angle position, are plotted against the crank angle position. Fig. 3 also shows the definition of SOC in terms of cumulative heat release rate in the case of a fuel showing clear two stage combustion. The point at which the second stage of combustion commences (SOC2) is also
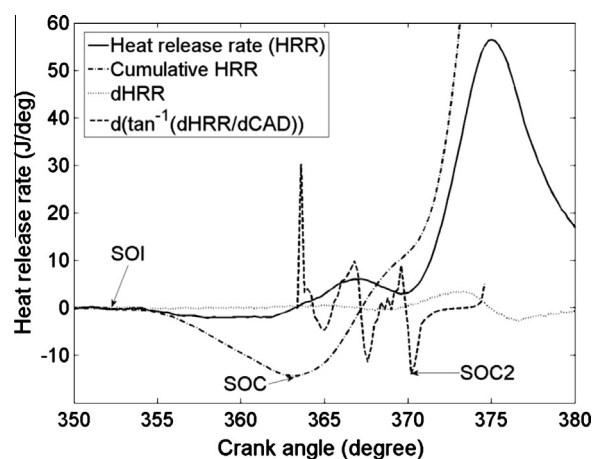
proportions with the reference fossil diesel. These experiments were performed at the same conditions of constant injection and constant ignition timing, but with no preheating of the fuel blends and with the low volume fuel system allowed to remain at ambient room temperature (~25 °C). Inlet air for these experiments was not heated. The tests with the fuel blends were also conducted at an engine speed of 1200 rpm, but at a lower fuel injection pressure of 450 bar. The injection duration was adjusted in the case of every fuel so that the engine IMEP was always constant at 4.00 bar for all blends. A summary of the engine and test operating conditions for these experiments is given in Table 6.

2.1.3.2. Spark ignition engine experiments. Following tests conducted in the compression ignition engine, three of the terpenes were tested as potential gasoline substitutes in the spark ignition engine. Geraniol, linalool and citronellene were blended in varying proportions with a reference fossil unleaded gasoline (RON 95), with the tests conducted at a spark timing of 26 or 30 CAD BTDC.

All tests were conducted at an engine speed of 1200 rpm with wide-open throttle (WOT) and with the carburetor set so that for all fuels the lambda value was always constant at a value of 1.00 ± 0.02. A summary of the engine and test operating conditions for these experiments is given in Table 7.

2.2. Synechocystis toxicity tests

2.2.1. Tolerance of Synechocystis to selected terpenes

Synechocystis sp. PCC6803 was cultured in shaker flasks in 25 ml of BG11 medium [28] at 25 °C with continuous illumination (~25 µE/m^2/s) and agitation (125 rpm). Aliquots of each of the five test compounds (geraniol, geranial, linalool, farnesene and citronelle) were added to individual flasks to a final concentration of 0.02%, 0.1%, 0.2%, 0.4% or 1% (v/v). The additions were done when cell growth was in the exponential phase and the population was approximately 7×10^7 cells/ml. Cultures with no added test compound were monitored to check viability during the course of the experiment. Photographs were taken every 24 h for 4 days to produce a visual series of culture viability.

2.2.2. Effect of a two-phase culture system on tolerance levels

Cultures (25 ml) were grown to a cell population of approximately 7×10^7 cells/ml before adding 0%, 0.02%, 0.04%, 0.08%, 0.1%, 0.2% and 1% v/v farnesene followed by 5 ml of *n*-dodecane to create an organic phase above the aqueous medium. Cultures with 0–1% v/v test compound were also grown in the absence of *n*-dodecane for comparison. Photographs of the cultures were taken every 24 h for 4 days.

Table 5
Single component fuels compression ignition engine and test operating conditions, where DNC denotes Did Not Combust.

Fuel	Engine speed (rpm)	Fuel injection pressure (bar)	IMEP (bar)	Constant injection timing (SOI at 7.5 CAD BTDC)				Constant ignition timing (SOC at TDC)			
				Ignition delay (CAD)		Injection duration (µs)		Ignition delay (CAD)		Injection duration (µs)	
				Mean	1 δ	Mean	1 δ	Mean	1 δ	Mean	1 δ
Reference fossil diesel	1200	700	4	5.0	0.1	589	13	4.8	0.2	590	14
Geraniol	1200	700	4	9.5	0.2	597	15	8.5	0.2	600	14
Nerol	1200	700	4	8.1	–	583	–	7.7	–	591	–
Citronellol	1200	700	4	8.5	–	618	–	8.7	–	624	–
3,7-Dimethyl-1-octanol	1200	700	4	7.9	–	596	–	7.8	–	603	–
Linalool	1200	700	4	DNC	–	–	–	DNC	–	–	–
Geranyl acetate	1200	700	4	8.4	0.1	637	5	8.2	0.1	642	5
Geranial (citral-A)	1200	700	4	5.5	–	598	–	5.1	–	601	–
Citral dimethyl acetal	1200	700	4	7.9	–	647	–	7.7	–	654	–
(−)-β-Citronellene	1200	700	4	DNC	–	–	–	13.6	–	596	–
ʟ-menthol	1200	700	4	DNC	–	–	–	9.3	–	596	–
Farnesene (mixture of isomers)	1200	700	4	6.5	–	566	–	6.4	–	571	–
Squalene	1200	700	4	6.7	–	598	–	6.7	–	591	–

Table 6
Terpene and reference diesel blends compression ignition engine and test operating conditions.

% Terpene in reference diesel (wt/wt)	Engine speed (rpm)	Fuel injection pressure (bar)	IMEP (bar)	Constant injection timing (SOI at 7.5 CAD BTDC)				Constant ignition timing (SOC at TDC)			
				Ignition delay (CAD)		Injection duration (µs)		Ignition delay (CAD)		Injection duration (µs)	
				Mean	1 δ	Mean	1 δ	Mean	1 δ	Mean	1 δ
0.0	1200	450	4.09 ± 2%	7.5	0.4	685	53	7.5	0.4	686	53
Farnesene											
5.0	1200	450	4.09	8.1	–	736	–	8	–	736	–
10.1	1200	450	4.09	8.5	–	735	–	8.3	–	737	–
20.3	1200	450	4.09	8.9	–	736	–	8.7	–	741	–
40.0	1200	450	4.09	10.1	–	737	–	9.9	–	735	–
51.2	1200	450	4.09	11.1	–	778	–	10.7	–	742	–
59.9	1200	450	4.09	DNC	–	–	–	10.9	–	751	–
Geranial											
7.8	1200	450	4.09	7.5	–	636	–	7.4	–	639	–
10.0	1200	450	4.09	7.5	–	640	–	7.6	–	642	–
20.3	1200	450	4.09	7.9	–	635	–	8.0	–	635	–
40.0	1200	450	4.09	8.9	–	644	–	9.0	–	647	–
50.0	1200	450	4.09	9.9	–	658	–	9.7	–	652	–
60.0	1200	450	4.09	10.1	–	677	–	10.1	–	655	–

Table 7
Terpene and reference gasoline blends spark ignition engine and test operating conditions.

% Terpene in reference gasoline (wt/wt)	Engine speed (rpm)	Lambda value (λ)	Throttle position	Spark timing (CAD BTDC)	IMEP (bar)		Knock frequency	
					Mean	1 δ	Mean	1 δ
0	1200	1.00 ± 0.02	WOT	26	10.48	0.11	3.80	1.44
Geraniol								
25.9	1200	1.00 ± 0.02	WOT	26	DNC	–	DNC	–
40.4	1200	1.00 ± 0.02	WOT	26	DNC	–	DNC	–
54.3	1200	1.00 ± 0.02	WOT	26	DNC	–	DNC	–
Citronellene								
28.8	1200	1.00 ± 0.02	WOT	26	10.24	0.04	1.81	0.19
45.2	1200	1.00 ± 0.02	WOT	26	10.47	0.33	1.77	0.16
0	1200	1.00 ± 0.02	WOT	30	10.17	–	23.17	–
Linalool								
10.7	1200	1.00 ± 0.02	WOT	30	10.81	–	1.00	–
37.5	1200	1.00 ± 0.02	WOT	30	10.40	–	16.67	–
64.8	1200	1.00 ± 0.02	WOT	30	10.49	–	2.00	–

3. Results and discussion

3.1. Compression ignition single component fuels

Fig. 4 shows the in-cylinder pressures and apparent net heat release rates of the terpenes and reference fossil diesel at constant injection and constant ignition timing. Linalool could not be induced to combust at either timing condition, while the remaining 11 single component fuels did combust at one or more of the timing conditions. The poor ignition quality of linalool is consistent with a previous study in which 2-decanol was found to exhibit a longer

ignition delay than 1-decanol [27]. While the terpenes exhibited a wide range of ignition delays, for all of the fuels (including the reference fossil diesel) the majority of heat release occurred during premixed combustion. Also visible in Fig. 4 is that several of the fuels exhibited significant cool flame combustion prior to peak heat release rates occurring. This is most prominent at constant ignition timing where menthol and citronellene in particular show limited heat release at TDC but the bulk of heat release does not then commence for approximately another seven CAD.

Fig. 5 shows the duration of the initial ignition delay period and the total duration of ignition delay of the terpenes and reference
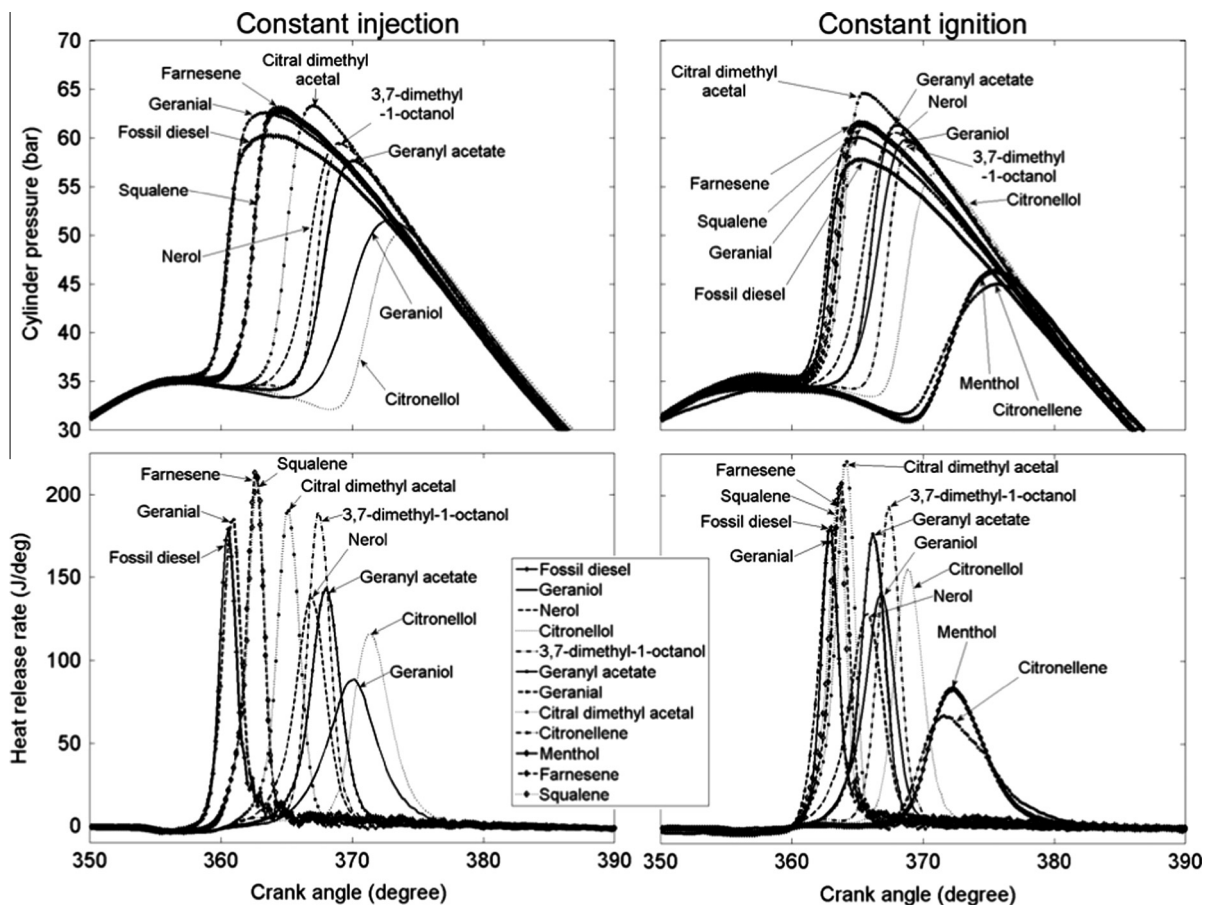

Fig. 4. In-cylinder pressures and apparent net heat release rates of the terpenes and reference fossil diesel at constant injection and constant ignition timing.

fossil diesel at constant injection and constant ignition timing. Where present in Fig. 5, and the following figures, the extent of the error bars given are plus and minus one standard deviation from the mean value (which is the point displayed on the plots) taken from repeat experimental runs of the same test fuel. The values of initial ignition delay presented in Fig. 5 are defined as the interval between SOI and the first appearance of positive apparent heat release for each fuel (SOC). The values of total ignition delay presented in Fig. 5 are defined as the interval between SOI and the point at which a second phase of heat release commences (SOC2 as defined in Section 2.1.3.1).

The low temperature reactions of molecules containing alkyl chains are well understood [29] and the effects of molecular structure on the rates of radical branching steps are apparent when considering the ignition delays of the terpenes. Geraniol displayed a greater initial ignition delay than the reference fossil diesel (Fig. 5), while nerol exhibited a slightly shorter initial ignition delay than geraniol (Fig. 5); this higher reactivity of the *cis* isomer is consistent with other studies of *cis* and *trans* isomers [30–32]. It also suggests that isomerization across the double bond of nerol in the *cis* arrangement is an important radical branching step, as it is known that such reactions can only occur with the double bond in the *cis* arrangement [30,33,34]. The significant difference (∼1 CAD) in the duration of initial ignition delay of geraniol at the two timing conditions (Fig. 5), is greater than for all other molecules tested and suggests a particular sensitivity of the low temperature kinetics of geraniol to in-cylinder conditions.

Reducing the number of double bonds present in the molecular structure, from two in geraniol to one in citronellol and none in 3,7 dimethyl-1-octanol (3,7-d-1-o), results in a linear decrease in initial ignition delay with increasing saturation at constant injection timing and a reduced ignition delay for only 3,7-d-1-o at constant ignition timing (Fig. 5). The effect of increasing ignition quality with higher levels of saturation has been observed previously in both straight alkyl chains [26] and fatty acid esters [35] and correlates with the ability of the molecule to undergo two important stages of low temperature radical branching. Namely, there is an increased availability of easily abstracted and weakly bonded secondary H atoms and there is increased potential of the alkyl chain to undergo internal isomerization [29], via the formation of six and seven member transition state rings (where the chain is formed of at least three saturated carbons [36]). However, when considering the total duration of ignition delay (Fig. 5), citronellol and 3,7-d-1-o

both possess a longer total duration of ignition delay than geraniol despite a shorter duration of initial ignition delay (Fig. 5). This implies that while in the case of citronellol and 3,7-d-1-o sufficient build up of radicals at low temperatures to initiate heat release occurs more quickly than geraniol, a longer 2nd period of ignition delay (SOC to SOC2) is required before a second autoignition event occurs and is able to propagate throughout the cylinder charge. It is tentatively put forward that this may be an effect of the viscosity of the terpenes, which is likely to influence the fuel droplet size and thus the efficiency of fuel and air mixing. In Table 3 it can be seen that at the test conditions of 60 °C, geraniol possesses a value of dynamic viscosity of 2.82 mPa s, citronellol 3.30 mPa s and 3,7-d-1-o 3.82 mPa s. Therefore it is suggested that a longer 2nd ignition delay period is required for citronellol and 3,7-d-1-o relative to geraniol as the rates of fuel and air mixing of the former are impeded by a higher fuel viscosity, and thus a critical amount of fuel and air mixture at suitable stoichiometry for ignition to escalate is arrived at more slowly. The longer total ignition delay of citronellol relative to 3,7-d-1-o (Fig. 5), despite a lower viscosity (Table 3), would seem to indicate that if the hypothesis is correct, then the importance of viscosity is no greater than that of the influence of molecular structure (Table 4) on low temperature reactivity.

Of the molecules which represent a change to the functional group of geraniol, geranial exhibits an ignition delay closest to that of the reference fossil diesel (with no significant 2nd ignition delay period), while citronellene possessed the longest initial and total ignition delay of any of the fuels tested (Fig. 5) and could only be induced to combust at constant ignition timing (Fig. 4). Furthermore, while fuels were considered to have not combusted (DNC) in the case of any misfire cycles, the combustion of citronellene was observed to be highly unsteady during engine tests. The shorter ignition delay of geranial relative to geraniol is consistent with cetane number measurements of the aldehyde octanal, which was found to possess a higher cetane number than the equivalent alcohol, octanol [31]. Aldehydes are known intermediates in the low temperature reactions of alcohols [37] and the high reactivity of such species can be attributed to the relative ease with which peroxy radicals may be formed, with only a single H atom to be abstracted and no addition of O required [38].

Geranyl acetate (Geranyl a.) and citral dimethyl acetal (Cda) possess a similar initial ignition delay that is shorter than that of geraniol but similar to that possessed by nerol (Fig. 5). Geranyl a. also displayed a total duration of ignition delay similar to nerol (Fig. 5) but that of Cda is slightly shorter. As previously discussed, an effect of viscosity on determining the duration of 2nd ignition delay is possible, with Cda possessing a lower viscosity than both geranyl a. and nerol (Table 3). However, nerol possesses a viscosity significantly greater than geranyl a. and displays a similar total ignition delay (Fig. 5). The poor ignition quality of citronellene (Fig. 5) relative to these molecules and the others of equal carbon number highlights the importance of the oxygenated functional groups relative to the unsaturated and branched alkyl moiety. Cetane number measurements of fully saturated and un-branched alcohols show them to possess approximately the same cetane number as un-branched 1-alkenes of equivalent carbon chain length and lower than that of *n*-alkanes of equivalent carbon chain length [31]. Therefore, it could be expected that an alcohol such as geraniol would be of lower ignition quality than the equivalent alkene, citronellene, whereas the opposite is true (Figs. 4 and 5). As citronellene possesses both the lowest viscosity (Table 2) and 2nd ignition delay period (Fig. 5) of all the fuels tested (Table 3), it would seem that any possible influence of fuel viscosity in determining the time of SOC2 is secondary to low temperature reactivity.

Farnesene and squalene were of similar ignition quality to one another and exhibited an initial ignition delay between that of
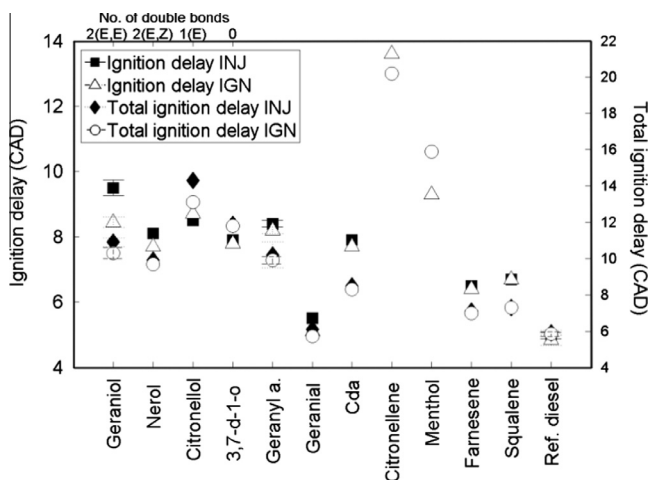

Fig. 5. Initial ignition delay (SOI to SOC) and total ignition delay (SOI to SOC2) of the terpenes and reference fossil diesel at constant injection (INJ) and constant ignition timing (IGN).

nerol and geranyl acetate (Fig. 5). However, the total duration of ignition delay of farnesene and squalene (Fig. 5) is only slightly greater than that of the reference fossil diesel and geranial. Citronellene, despite an overall shorter carbon chain length, possess a longest saturated alky chain equal in length to that possessed by the farnesene and squalene. Therefore, the shorter ignition delay of farnesene and squalene relative to citronellene suggests that reactions involving the unsaturated portions of the alkenes are significant low temperature branching routes. The only cyclic molecule tested, L-menthol, could not be induced to combust at constant injection timing (Fig. 4) and at constant ignition timing exhibited an ignition delay slightly greater than that exhibited by geraniol (Fig. 5) and the longest total duration of ignition delay of all molecules except citronellene (Fig. 5).

Fig. 6 shows the peak apparent heat release rate and time of peak apparent heat release rate of the terpenes and reference fossil diesel at both timing conditions. For those molecules that exhibited a total ignition delay (Fig. 5) less than 8 CAD, there is a clear trend of increasing peak heat release rate (Fig. 6) with increasing duration of total ignition. This can be attributed to the longer duration available for fuel and air mixing prior to SOC2 resulting in more combustible fuel air mixture available at ignition and thus a higher peak heat release rate. This is consistent with a previous study of n-alkanes and alkenes in which a very strong correlation was found between the duration of ignition delay, the extent of the premixed burn fraction and the peak heat release rate [26].

For those molecules which exhibited a longer ignition delay than 8 CAD, the inverse relationship between ignition delay and peak heat release rate becomes apparent; that is, the longer the duration of total ignition delay (Fig. 5) and thus the later the time of peak heat release rate (Fig. 6), the lower the magnitude of peak heat release rate (Fig. 6). This is especially apparent in the case of citronellene and menthol which display the lowest peak heat release rates (Fig. 6) of all the fuels tested despite possessing the longest durations of total ignition delay (Fig. 5). It follows that with the time of peak heat release rate (Fig. 6) for these molecules occurring later into the expansion stroke, a greater degree of heat transfer to the cylinder walls could be expected and thus result in lower values of apparent heat release rate (where heat transfer has not been accounted for). Similarly, Cda displays a higher peak heat release than those molecules with a longer ignition delay by virtue of a time of peak heat release rate closer to TDC (Fig. 6). This effect of cylinder volume at the time of peak heat release rate can also account for the differing peak heat release rates observed for tests

conducted at constant ignition timing relative to those conducted at constant injection timing (Fig. 6).

Fig. 7 shows the calculated maximum in-cylinder global temperature and the time of occurrence of the terpenes and reference fossil diesel at both timing conditions. It could be expected that those fuels that exhibited the highest peak heat release rates would also show the highest global maximum in-cylinder temperatures. However, such an influence is only visible for those fuels with a total ignition delay (Fig. 5) less than 8 CAD, citronellene, menthol and also Cda, which exhibits both the highest peak heat release rate (Fig. 6, constant ignition timing only) and maximum in-cylinder temperature (Fig. 7). Geraniol, nerol, citronellol, and geranyl a. all show a higher maximum in-cylinder temperature (Fig. 7) than geranial, farnesene and squalene despite possessing similar or lower peak heat release rates (Fig. 5). Nor does the time of maximum in-cylinder global temperature (Fig. 7) mirror the time of peak heat release rate (Fig. 6) as closely as might be expected. However, there is a consistent effect of injection timing; at constant injection timing geraniol displayed both a lower peak heat release rate (Fig. 6) and maximum in-cylinder temperature (Fig. 7) that occur later into the expansion stroke (Figs. 6 and 7), than at constant ignition timing. It is suggested that this lack of a clear trend in maximum in-cylinder temperature highlights the
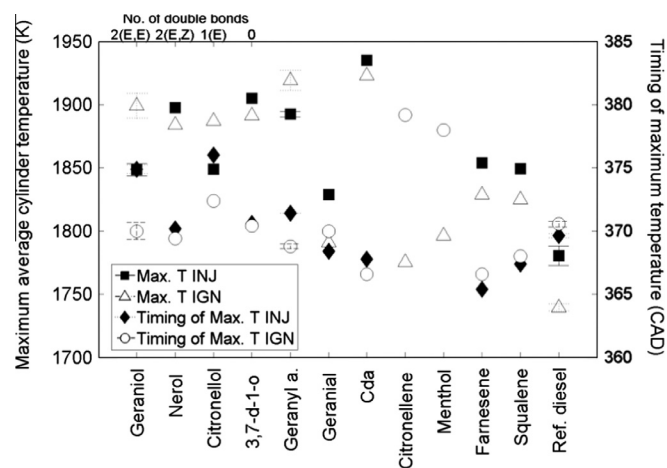
Fig. 7. Calculated maximum in-cylinder global temperature (Max. *T*) and (b) time of occurrence of the terpenes and reference fossil diesel at constant injection (INJ) and constant ignition timing (IGN).
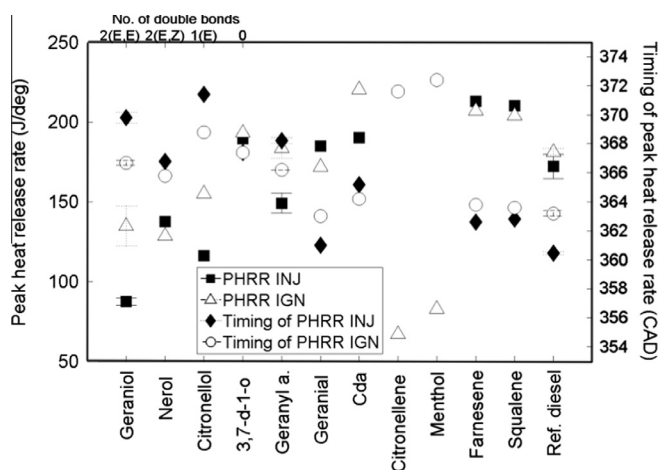
Fig. 6. Peak apparent heat release rate (PHRR) and time of peak apparent heat release rate of the terpenes and reference fossil diesel at constant injection (INJ) and constant ignition timing (IGN).
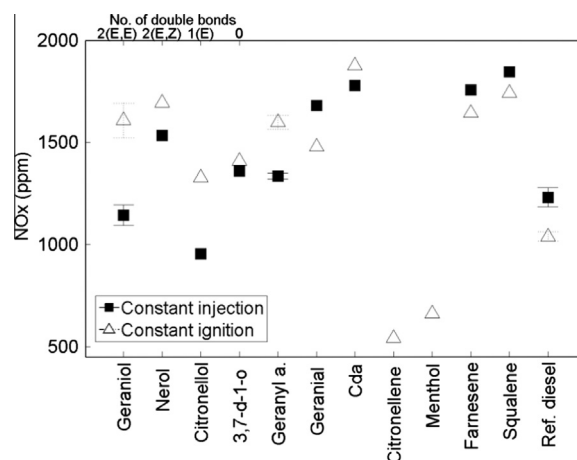
Fig. 8. Exhaust NOx emissions of the terpenes and reference fossil diesel at constant injection and constant ignition timing.

sensitivity of in-cylinder thermal conditions to the volume at which they occur, as differences in cylinder volume will be more significant for those fuels which displayed a total ignition delay of less than 8 CAD (Fig. 5) where SOC and SOC2 occur further away from TDC.

Fig. 8 shows the NOx exhaust levels of the terpenes and reference fossil diesel at both timing conditions. At constant injection timing, all of the fuels except geraniol and citronellol produced higher NOx emissions than the reference diesel, while at constant ignition timing all of the fuels except citronellene and menthol emitted higher levels of NOx than the reference diesel (Fig. 8). The production of NOx in diesel combustion is known to be highly thermally sensitive [39], both to the magnitude of the in-cylinder temperature and the residence time of the cylinder contents at elevated temperatures [35,40,41]. An influence of both is apparent in the levels of NOx emitted, for example the lowest NOx levels were emitted by citronellene and menthol (Fig. 8), despite both exhibiting a higher maximum in-cylinder global temperature than the reference fossil diesel (Fig. 7). This can therefore most likely be attributed to the timing of the maximum in-cylinder temperature (Fig. 7), which is significantly later for both citronellene and menthol, thus resulting in a shorter duration of time at which the cyl-

inder contents are at a sufficiently high temperature for NOx production. The same two mechanisms appear to also be responsible for the differing levels of NOx emitted at the two timing conditions for some fuels. For example, geraniol produced significantly higher levels of NOx at constant ignition timing relative to constant injection timing; the calculated maximum in-cylinder temperature at constant injection timing was lower and occurred later. The importance of peak heat release in determining NOx emissions is also apparent; both farnesene and squalene emit similar levels of NOx as Cda despite a lower maximum in-cylinder temperature (Fig. 7) occurring only slightly earlier, but do exhibit a similar peak heat release rate (Fig. 6). This is perhaps indicative of the limitations of calculated maximum in-cylinder global temperature in understanding conditions within local combustion zons.

Figs. 9a and b show the exhaust gas levels of CO and THC of the terpenes and reference fossil diesel at both timing conditions. The highest levels of CO and THC were both emitted by citronellene and menthol (Figs. 9a and b), which suggests the presence of both fuel rich and fuel lean regions during combustion. Geraniol and citronellol both produced significantly more CO at constant injection timing (Fig. 9a), at which condition both fuels also exhibited a lower maxium in-cylinder temperature (Fig. 7) and thus suggests that
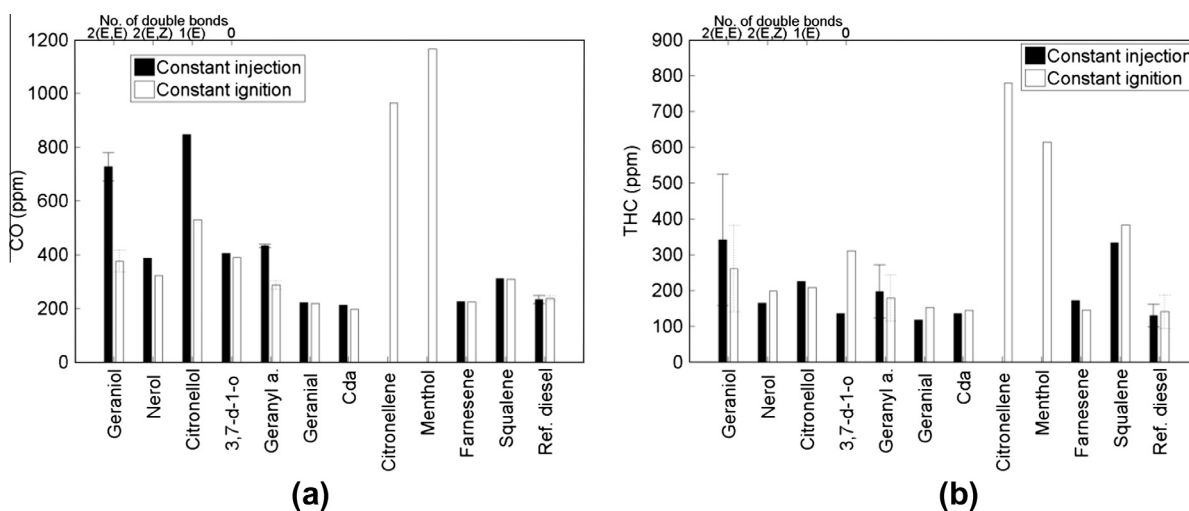

Fig. 9. (a) CO and (b) THC emissions of the terpenes and reference fossil diesel at constant injection and constant ignition timing.
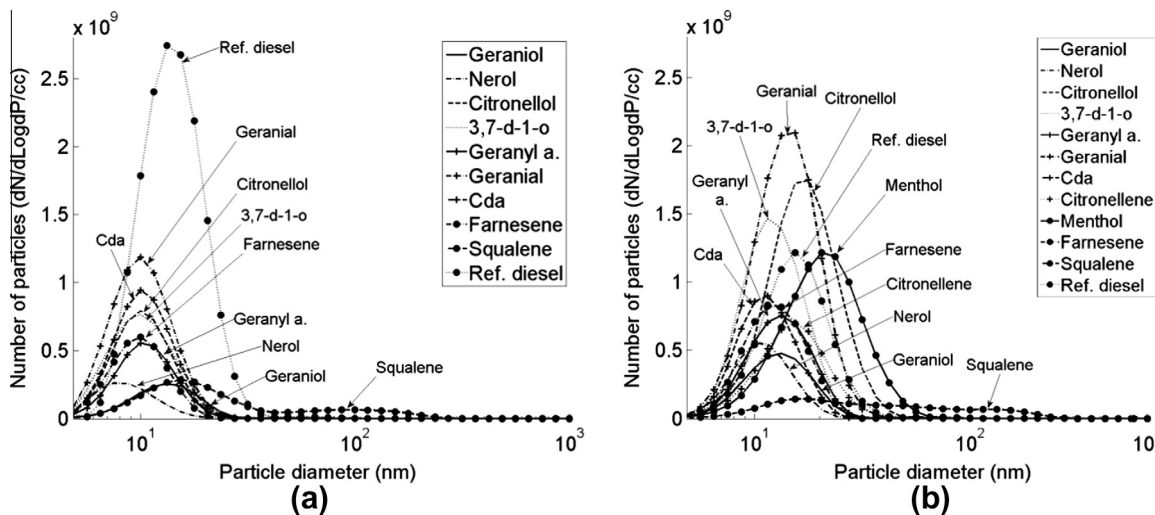

Fig. 10. Particulate emissions of the terpenes and reference fossil diesel at (a) constant injection timing and (b) constant ignition timing.

lower temperatures resulted in a greater degree of incomplete combustion. At both timing conditions squalene emitted higher levels of THC than farnesene (Fig. 9b) despite both fuels exhibiting broadly similar combustion characteristics; however, the range of error presented in Fig. 9b is also significant.

Figs. 10a and b show the particulate number distribution of the terpenes and reference fossil at both timing conditions. At constant injection timing the most significant peak in nucleation mode particles (Dp <50 nm) is displayed by the reference fossil diesel
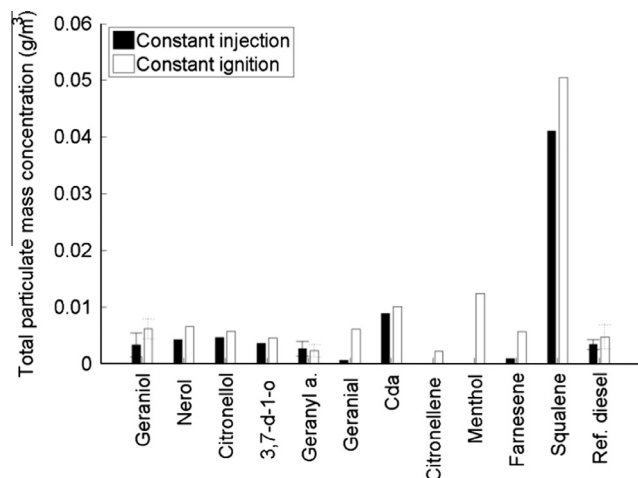
(Fig. 10a) with the terpenes exhibiting considerably smaller peaks in the same size range (~1E9 vs 2.7E9). At constant ignition timing the peak in nucleation mode particles displayed by several of the terpenes increased, while that displayed by the reference fossil diesel decreased (Fig. 10b). Of the oxygenated molecules tested, at both timing conditions, geraniol and nerol displayed the lowest peaks in nucleation mode particles (Figs. 10a and b).

Considering larger accumulation mode particles (Dp >50 nm), these were produced in far greater abundance by squalene than any other fuel at both timing conditions (Figs. 10a and b). Squalene possesses the highest viscosity of all the fuels tested (Table 3) by a considerable margin to the next most viscous, 3,7-d-1-o (6.17–3.82 mPa s) and thus fuel droplets of squalene prior to combustion and during mixing with air are likely to be larger than those of the other fuels. It is suggested that this results in the high production of accumulation mode particles observed by increasing the presence of fuel rich zones (with larger droplet sizes impeding fuel and air mixing) which are conducive to the production of soot [42], and may also explain the higher emissions of CO and THC of squalene relative to farnesene (Figs. 9a and b).

Fig. 11 shows the total mass of particulates emitted by the terpenes and reference fossil diesel. At both timing conditions, squalene produced a significantly greater total mass of particulates than any of the other fuels tested (Fig. 11). This can be attributed to the higher number of accumulation mode particles produced by squalene relative to the other fuels (Figs. 10a and b). After squalene, menthol and Cda emitted the next highest mass concentrations of soot; this could be expected from the former as cyclic structures are know for a higher propensity to form soot [43] but less so the later, the high oxygen content and calculated maximum

Fig. 11. Total mass of particulates emitted in the exhaust gas of the terpenes and reference fossil diesel at constant injection and constant ignition timing.
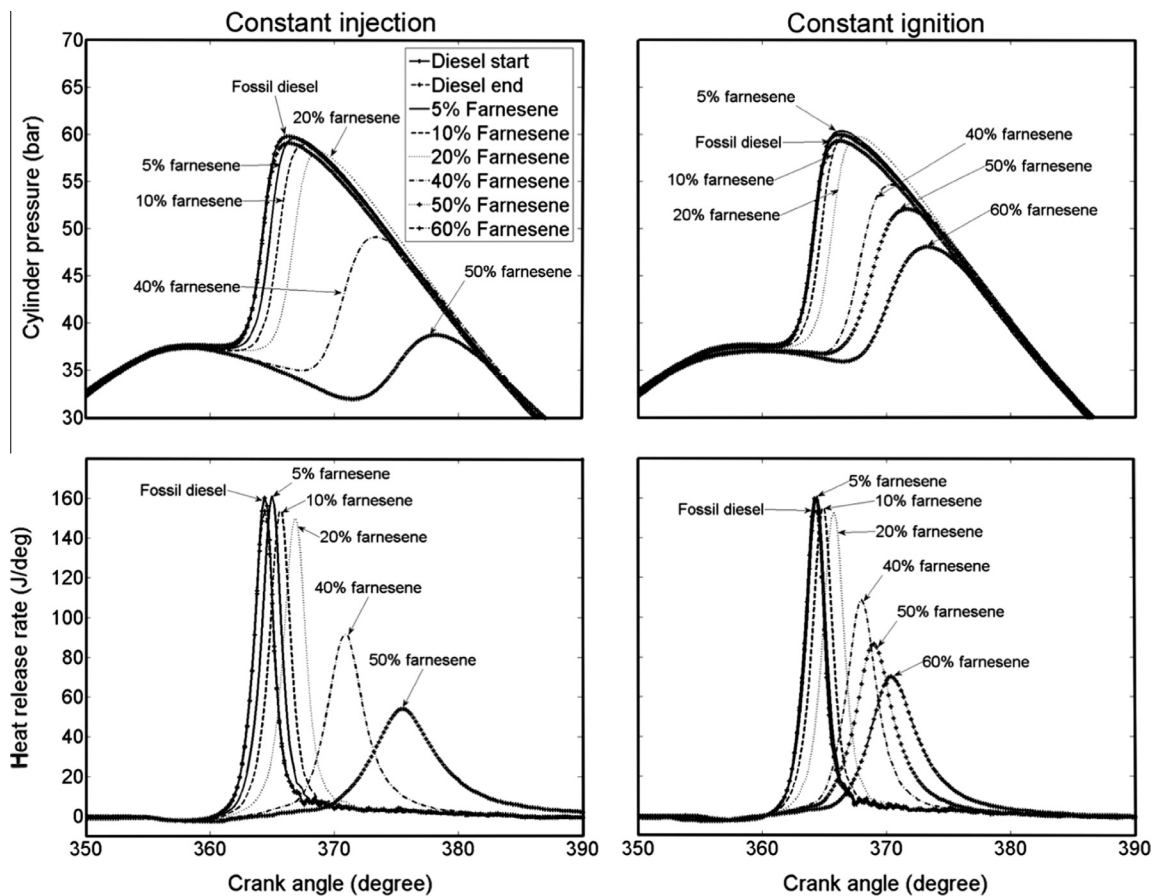

Fig. 12. In-cylinder pressures and apparent net heat release rates of the farnesene and reference fossil diesel blends at constant injection and constant ignition timing.

in-cylinder global temperature of which could both be expected to increase soot oxidation [42]. All of the other terpenes tested produced an equivalent or lower amount of soot than geraniol (Fig. 11), however the range of error encountered makes further characterization somewhat difficult.

3.2. Compression ignition terpene and reference fossil diesel blends

Testing of the terpenes as pure components (Section 3.1) revealed geranial and farnesene to be the most promising in terms of both combustion characteristics and production of emissions. Therefore, a further series of experiments was conducted in which both geranial and farnesene were blended with the reference fossil diesel in varying proportions and tested in the engine at less extreme operating conditions (Section 2.1.3.1). Figs. 12 and 13 show the in-cylinder pressures and apparent hear release rates of both the farnesene and geranial blends with reference fossil diesel at constant injection and constant ignition timing. Both terpenes could not be induced to combust at the experimental conditions (Section 2.1.3.1 and Table 6) at blend levels greater than 60% with the reference fossil diesel, at either timing conditions. Apparent, from both Figs. 12 and 13, is a reduction in the premixed burn fraction and a more pronounced period of 2nd ignition delay (with a latter time of peak heat release rate) when either terpene is blended with the reference fossil diesel in concentrations greater than 20%. It is interesting to note that both geranial and farnesene combusted as single components with a similar, or not significantly longer, ignition delay than the reference fossil diesel under the conditions of elevated fuel and inlet air temperature and higher injection pressure (Section 2.1.3.1 and Table 5). Geranial and farne-

sene possess a lower viscosity than the reference fossil diesel at both 20 °C and 60 °C (Table 3), so it would seem unlikely that the greater reactivity of the terpenes can be attributed to a change in physical properties and the efficiency of fuel and air mixing. Therefore, it would seem that for pure geranial and farnesene, the extra kinetic and thermal energy provided by the elevated air and fuel temperatures and injection pressure activates radical branching routes that are not available at the lower energy input conditions used in the tests of the terpenes as blends with reference fossil diesel. For the reference fossil diesel, while ignition delay is reduced at the elevated temperature and injection pressure conditions (Tables 5 and 6) the change in reactivity is much less pronounced.

Figs. 14a and b show the initial ignition delay (SOI to SOC) and coefficient of variation in ignition delay of the terpene and reference fossil diesel blends at both timings. There is a near linear increase in the initial ignition delay of the blends with the increasing terpene component (Fig. 14a), while the stability of combustion (as indicated by the coefficient of variation of ignition delay) decreases appreciably for blends of greater than 40% terpene (Fig. 14b) and coincides with visibly much longer periods of 2nd ignition delay (Figs. 12 and 13). This is consistent with engine studies of ethanol blended with fossil diesel (the low ignition quality of which results in it being an unsuitable single component fuel for normal compression ignition combustion [31]), which also increased cycle to cycle variability when present at increasing levels [44,45]. While at constant ignition timing, the effect of both geranial and farnesene on ignition delay was similar, at constant injection timing the geranial blends with fossil diesel generally had a slightly shorter ignition delay than those comprising of farnesene and the fossil diesel in the same proportions (Fig. 14a).
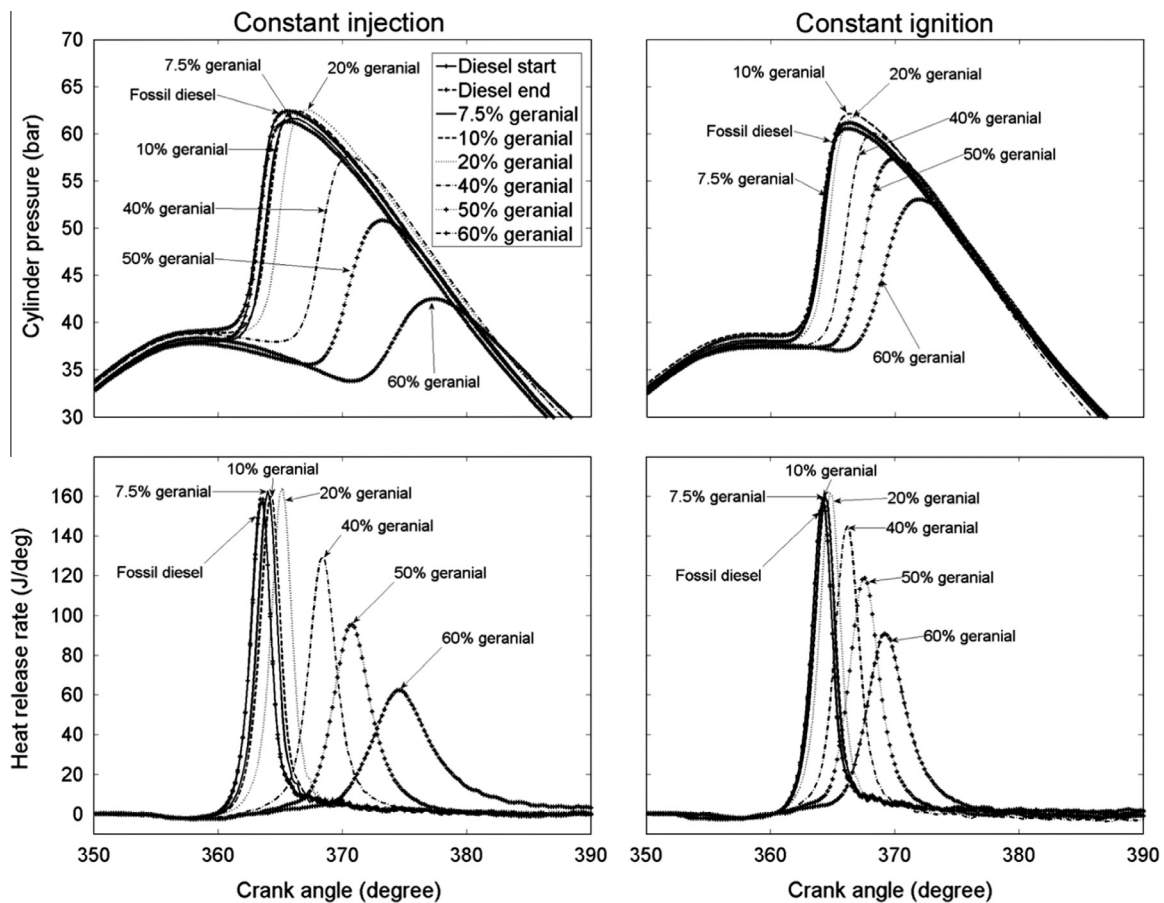

Fig. 13. In-cylinder pressures and apparent net heat release rates of the geranial and reference fossil diesel blends at constant injection and constant ignition timing.
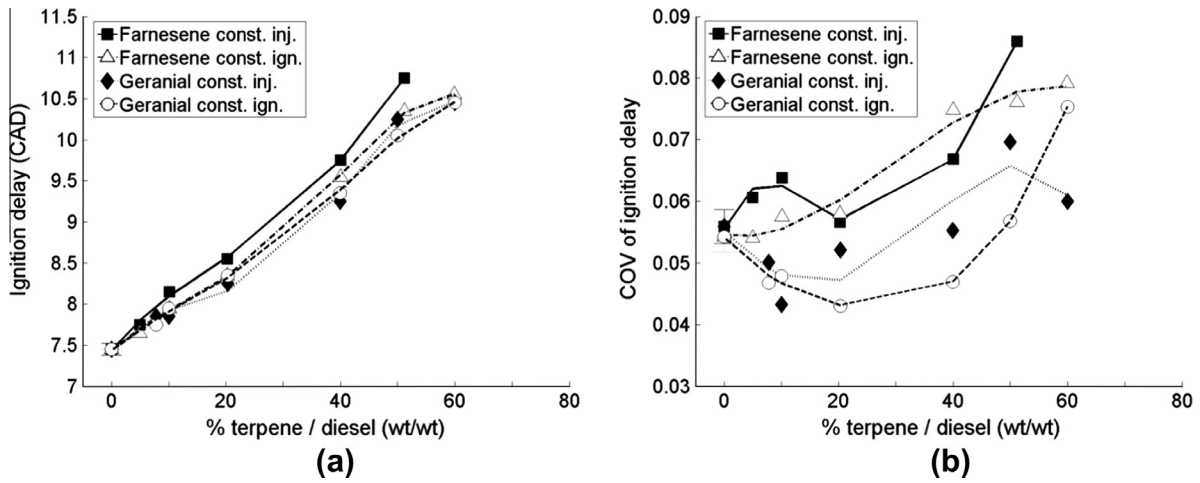
Fig. 14. (a) Ignition delay and (b) coefficient of variation in ignition delay of the terpene and reference fossil diesel blends at constant injection and constant ignition timing.

Figs. 15a and b show the peak apparent heat release rate and the calculated maximum in-cylinder global temperature of the terpene and reference fossil diesel blends at both timings. The increase of either terpene in the blend results in both a decrease in the peak heat release rate (Fig. 15a) and the calculated maximum in-cylinder temperature (Fig. 15b). Both trends are significant only after the terpene is present at 20% or greater (Figs. 15a and b) and the occurrence of peak heat release rate significantly further into the expansion stroke was observed (Figs. 12 and 13). A correlation with ignition delay is readily apparent; blends of farnesene with fossil diesel at constant injection timing, which possessed the longest relative ignition delays for equivalent terpene content (Fig. 14a), show the steepest decrease in both peak heat release rate (Fig. 15a) and maximum in-cylinder global temperature (Fig. 15b).

Fig. 16 shows the exhaust gas levels of NOx for the terpene and reference fossil blends at both timing conditions. A strong correlation between the levels of NOx emitted (Fig. 16) and the magnitude and time of occurrence of maximum in-cylinder temperature reached (Figs. 15a and b) is readily apparent. Any influence of fuel oxygen content would appear to be secondary to the in-cylinder thermal conditions and is not visible as the increasing availability of oxygen might be expected to result in increasing NOx emissions with terpene content, whereas the opposite is true.

Figs. 17a and b show the CO and THC emissions of the terpene and reference fossil diesel blends at both timing conditions.
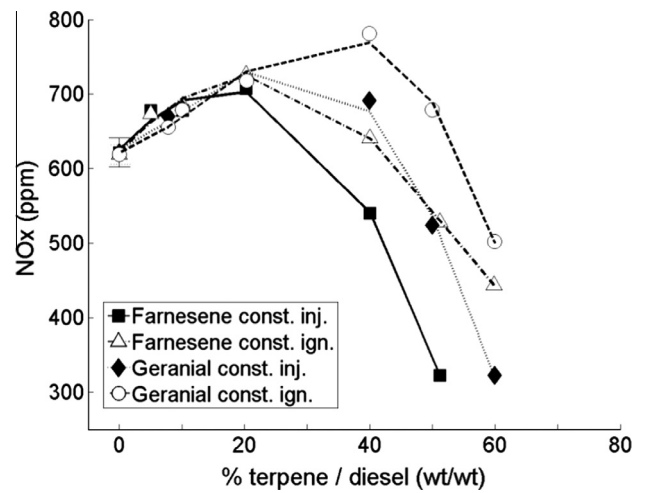

Fig. 16. NOx emissions of the terpene and reference fossil diesel blends at constant injection and constant ignition timing.
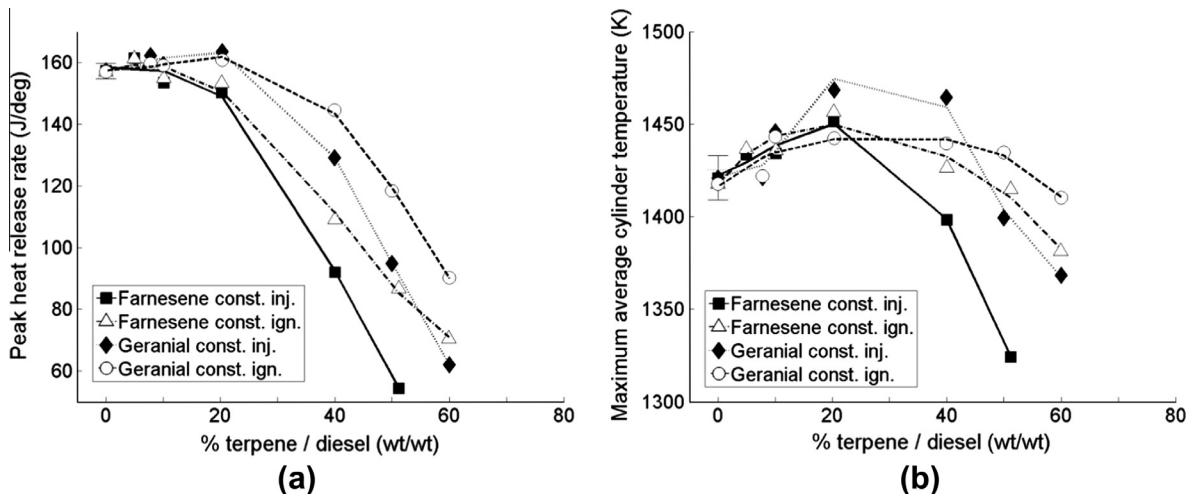

Fig. 15. (a) Peak apparent heat release rate and (b) calculated maximum in-cylinder global temperature of the terpene and reference fossil diesel blends at constant injection and constant ignition timing.

Exhaust gas levels of CO and THC increase with the level of terpene present in the fuel blend, though levels of both are consistently higher at constant injection timing relative to constant ignition timing (Figs. 17a and b). The farnesene blends produced higher CO emissions (Fig. 17a) than those of geranial at both timing conditions, but only produced higher emissions of THC in the case of the blend containing 50% farnesene at constant injection timing. As was observed in the combustion of citronellene and menthol (Figs. 9a and b), the concurrent emission of high levels of THC and CO indicates the presence of both fuel lean and fuel rich areas within the cylinder charge (Figs. 17a and b). An influence of in-cylinder thermal conditions via the peak heat release rate (Fig. 15a) is readily apparent in the levels of CO emitted (Fig. 17a). The blends of farnesene at constant injection timing display the lowest peak heat release rates (Fig. 15a) and the highest emissions of CO (Fig. 17a) for a given terpene content, while blends of geranial at constant ignition timing show both the highest peak heat release rates and lowest CO emissions for a given terpene content.

Figs. 18a and b and 19a and b, show the particulate emissions of the farnesene and geranial blends with reference fossil diesel at both timing conditions. At constant injection timing, for both blends of farnesene and geranial, the blends with the highest terpene content produced the largest peak in nucleation mode parti-cles (Figs. 18a and 19a). In the case of the geranial blends, there is a suggestion from Fig. 19a that the peak number of nucleation mode particles produced decreases with the geranial content of the fuel blend. This is not apparent in the case of the farnesene blends (Fig. 18a). At constant ignition timing (Figs. 18b and 19b), the peak levels of nucleation mode particles produced by the highest terpene content blends are lower relative to the peaks observed at constant injection timing (Figs. 18a and 19a). Furthermore the range of peaks produced is narrowed with the experimental error (as indicated by repeat data of pure fossil diesel) remaining similar. The high levels of THC displayed by those blends with the highest terpene content (Fig. 17b), potentially suggest that a portion of the nucleation mode particles measured are in fact droplets of un-burnt fuel.

Fig. 20 shows the total mass of particulates produced by the terpene and reference fossil diesel blends at both timing conditions. It is not possible to discern any particular influence of the level of terpene present on the production with the range of error present in Fig. 20. However, it is tentatively suggested that this is itself a useful observation as no significant increase in soot production was noted with the highest concentration terpene blends despite lower temperature (Fig. 15b) and possible fuel rich conditions (Fig. 17a) which might normally be considered conducive to the formation of soot particles [42].
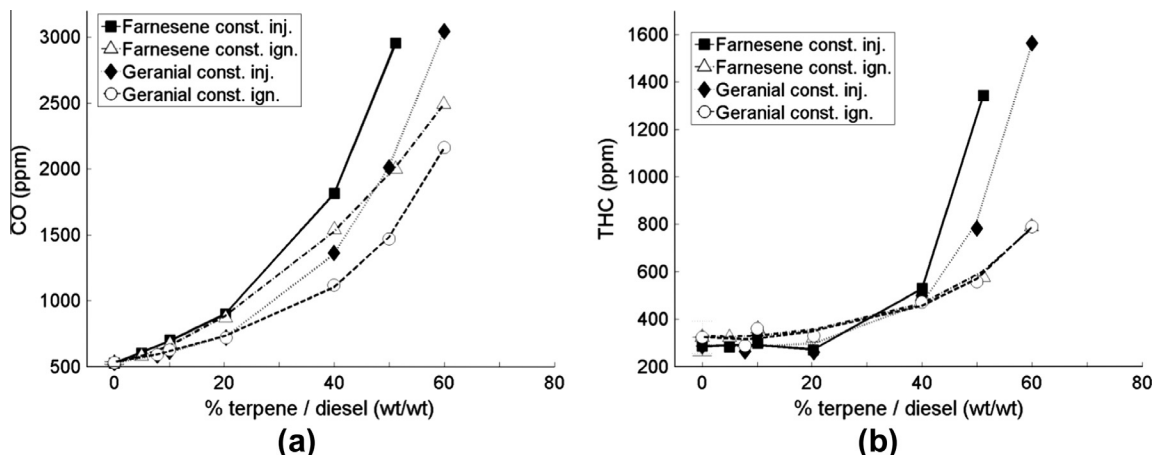

Fig. 17. (a) CO and (b) THC emissions of the terpene and reference fossil diesel blends at constant injection and constant ignition timing.
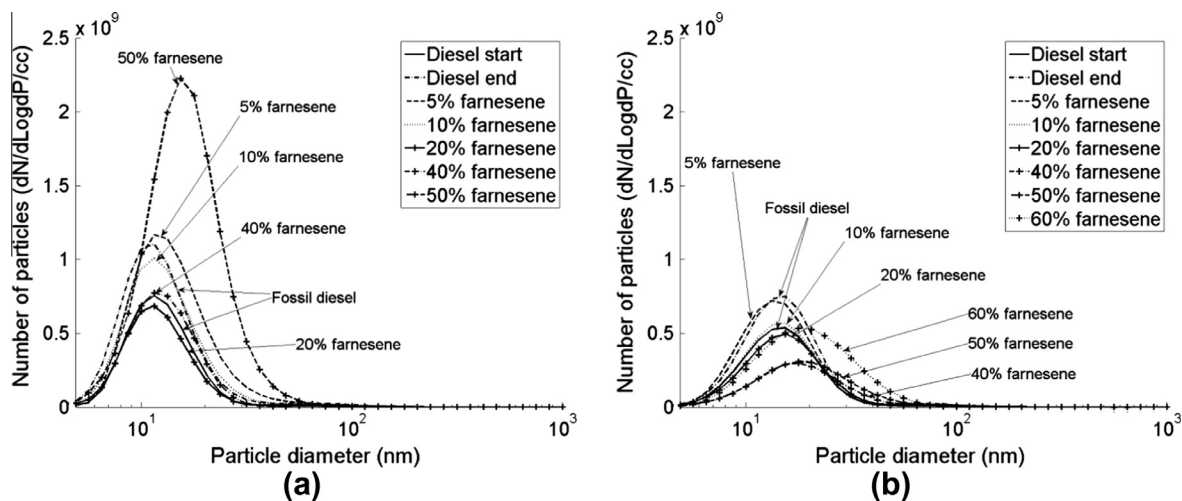

Fig. 18. Particulate emissions of farnesene and reference fossil diesel blends at (a) constant injection timing and (b) constant ignition timing.
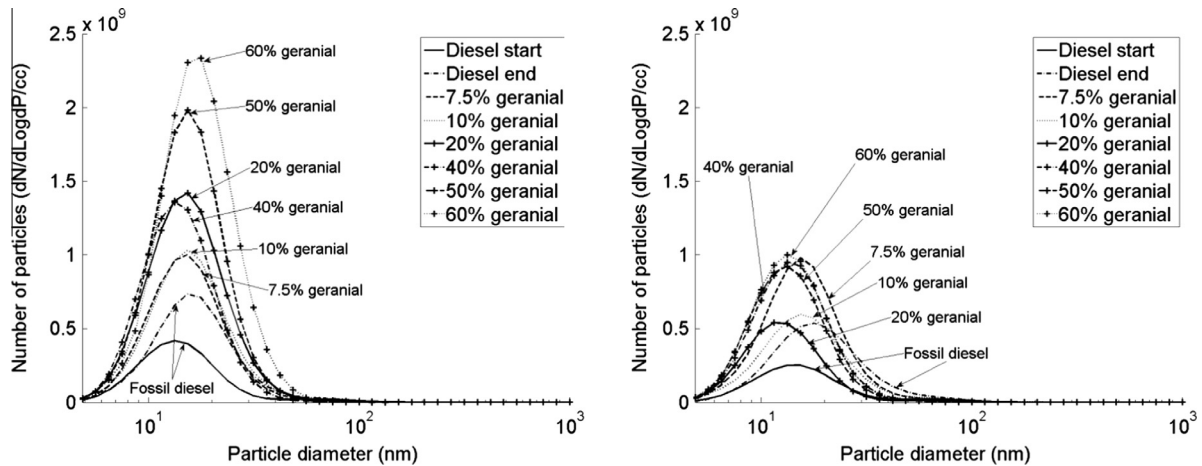
Fig. 19. Particulate emissions of geranial and reference fossil diesel blends at (a) constant injection timing and (b) constant ignition timing.

3.3. Spark ignition engine terpene and reference gasoline blends

A further series of experiments was conducted in a spark ignition engine to assess the performance of citronellene and linalool which, by virtue of being exceptionally poor compression ignition fuels, would potentially prove better suited to spark ignition. Geraniol was also to be assessed but found not to be readily soluble with fossil gasoline, and mixtures of both would not remain stable for sufficient periods of time in which to conduct the engine experiments. Citronellene and linalool were, however, found to be soluble and stable in fossil gasoline up to a content of 45% and 65% (wt/wt) respectively.

Figs. 21a and b show the average IMEP (mean of 300 cycles) and knock frequency (% cycles) for the terpene and fossil gasoline blends. In Figs. 21–23, all data has been normalised for a constant spark ignition time of 26 CAD BTDC. With the range of error presented, it is difficult to discern a clear effect of adding either terpene on the average IMEP (Fig. 21a). However, it is of interest to note that in the case of the blend of 45% citronellene with fossil gasoline the magnitude of this error is significantly larger than of pure fossil gasoline or the blend of 29% citronellene, suggestive of less steady combustion. Notwithstanding the extent of error presented, there is a suggestion that the addition of linalool to fossil gasoline increased IMEP, whereas the addition of citronellene did not (Fig. 21a). The knock frequency presented in Fig. 21b was
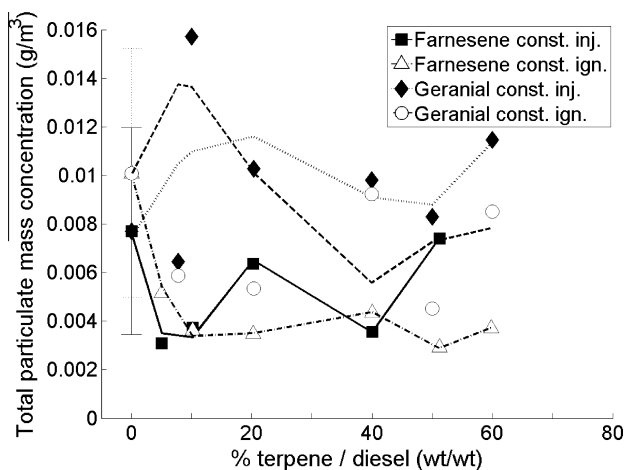
determined by the application of a bandwidth filter of 4–7 kHz to the in-cylinder pressure data to detect knock events above a constant intensity threshold. In Fig. 21b, it can be seen that increasing the level of either terpene in the blend with fossil gasoline reduced propensity to knock; though a significant level of cycle-to-cycle variation is visible. This is not unexpected; as pure components, both terpenes proved to be poor diesel fuels (Table 5 and Fig. 4) and as such proved themselves resistant to auto-ignition.

Fig. 22 shows the flame front development angles (0–10% mass fraction burnt) for the terpene and fossil gasoline blends. For all blends the flame front development angle is between 32 and 36 CAD and at the test conditions employed (Table 7) shows that combustion occurred near TDC for all blends. In the case of the citronellene and fossil gasoline blends no significant impact of terpene content of the flame front development angle can be observed, though as when considering the average IMEP (Fig. 21a), combustion of the mixture containing 29% citronellene would appear more steady than that containing 45% citronellene, as indicated the by the size of the respective error bars (Fig. 22). Addition of linalool to gasoline would appear to decrease the flame front development angle (Fig. 22), most severely for the blend containing 10% linalool and progressively less so as the linalool content is increased to 65%. This mirrors the trend apparent in IMEP (Fig. 21a) in which the blend containing 10% linalool displayed the highest IMEP of all blends tested.

Figs. 23a and b show the peak heat release rate and time of occurrence for the terpene and fossil gasoline blends. Peak heat release rates (Fig. 23a) show a correlation with average IMEP (Fig. 21a), which is to be expected when combustion of all blends is occurring near TDC and at similar cylinder volumes. The timing of peak heat release rate (Fig. 23b) correlates well with the flame front development angle (Fig. 22) and suggests that combustion of all the terpene and fossil gasoline blends commences at a similar rate once the flame front has propagated throughout the cylinder charge. It is difficult to discern a clear effect of increasing the content of citronellene on either peak heat release rate (Fig. 23a) or the time at which it occurs (Fig. 23b), however, the relative size of the error bars presented again indicates the combustion of the mixture containing 45% citronellene to be somewhat less steady than that containing 29% of the same terpene. Addition of 10% linalool to the reference fossil gasoline would appear to increase combustion rates, with both a higher peak heat release rate (Fig. 23a) than pure fossil gasoline and an earlier time of occurrence (Fig. 23b). However, further addition of linalool results in no significant net change in either peak heat release or its timing relative to pure fossil gasoline. The higher peak heat release rate of the 10% linalool blend

Fig. 20. Total mass of particulates emitted in the exhaust gas of the terpene and reference fossil diesel blends at constant injection and constant ignition timing.
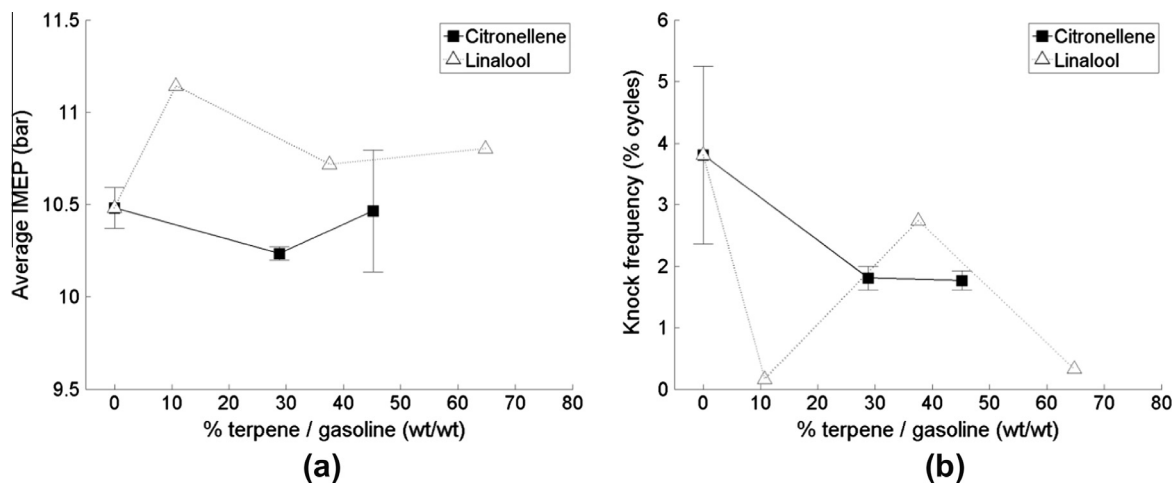
Fig. 21. (a) Average IMEP and (b) knock frequency of terpene and fossil gasoline blends.

(Fig. 23a) is in agreement with the observed higher IMEP of the same blends (Fig. 21a), and is suggestive of a non-linear effect on

Fig. 22. Flame front development (0–10% mass fraction burnt) angle of terpene and fossil gasoline blends.

Fig. 23. (a) Peak apparent heat release rate and (b) time of occurrence of terpene and fossil gasoline blends.

combustion of increasing the level of linalool present; however, the absence of error bars for this mixture should be noted.

3.4. Cyanobacterial toxicity tests

The tolerance of *Synechocystis* to geraniol, geranial, linalool, far-nesene and citronellene was investigated in liquid cultures by monitoring whether addition of the compound inhibited further growth and led to bleaching of the culture. As seen in Fig. 24, gera-niol and geranial had the most toxic effects on *Synechocystis* even after just 24 h of addition as indicated by the almost complete loss of pigmentation even at the lowest concentration of 0.02% (v/v). Linalool was less toxic than geraniol and geranial at the lower con-centrations (0.02%) while the cyanobacterium was able to tolerate the highest concentration (1%) of both farnesene and citronellene, suggesting that biosynthesis of these two compounds in geneti-cally engineered strains should not prove toxic, at least at this concentration.

Fig. 25 shows the same experiment after 4 days. It is clear that the cultures are unable to recover from the addition of geraniol or geranial, even at the lowest concentration. The death of the cells was confirmed by plating aliquots from the 0.02% geraniol flask onto solid medium, and observing that no colonies appeared fol-lowing incubation. Whilst reduced growth is observed for 0.02% linolool and farnesene, higher concentrations appear toxic despite
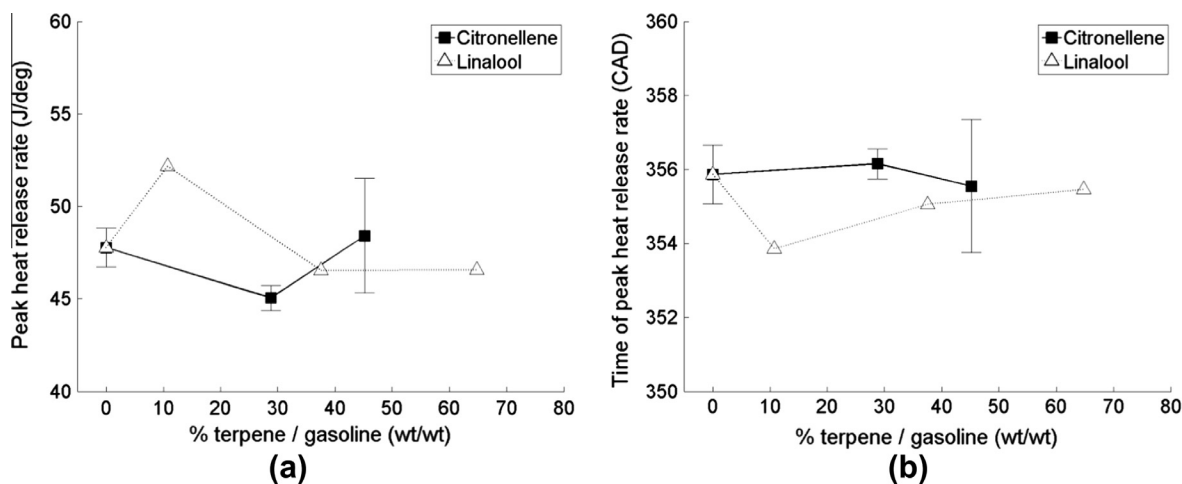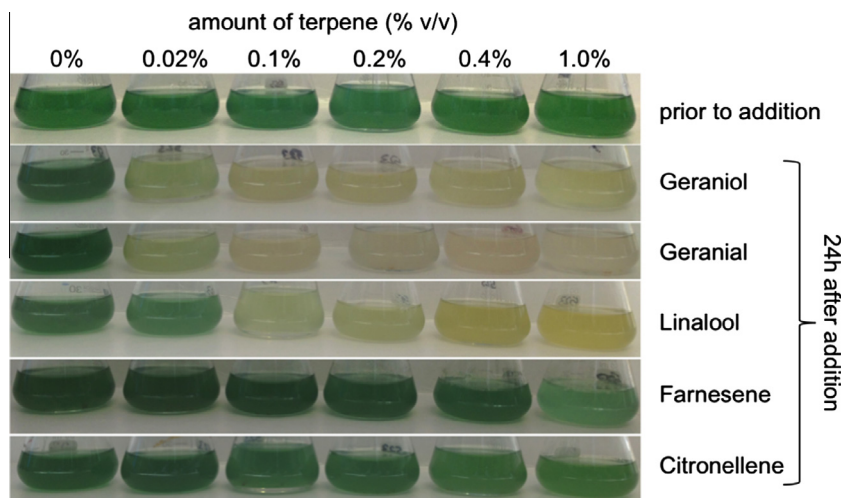
Fig. 24. The tolerance of *Synechocystis* to increasing amounts of the five test compounds 24 h after addition.

the promising observation for farnesene at 24 h (Fig. 24). The least toxic compound is citronellene and healthy growth of *Synechocystis* is seen even after 4 days exposure to the highest concentration (1%).

The toxic effect of terpenes on *Synechocystis* was expected, as it is well documented that many terpenes display antimicrobial properties [46–50]. For example, studies on another Gram-negative bacterium, namely *E. coli*, have shown that geranial and geraniol inhibit growth at concentrations higher that 0.05% [48,51]. The toxicity of a terpene is correlated with how well it partitions in the cell membrane and recently there have been several efforts towards genetically engineering microorganisms to better tolerate such molecules [51]. However, an alternative strategy is the addition of a non-toxic organic solvent to the culture medium to form a

two-phase system in which the toxic product is 'milked' from the cells and accumulates in the organic phase [22]. This would reduce accumulation in the aqueous phase and keep levels below the toxicity threshold. Fig. 26 demonstrates the effect of adding *n*-dodecane to the culture medium, and compares cultures of *Synechocystis* inoculated with 0%, 0.02%, 0.04%, 0.08%, 0.1%, 0.2% and 1% v/v farnesene grown in the presence and absence of *n*-dodecane. The flasks containing *n*-dodecane showed a marked improvement in survival after 4 days (Fig. 26), even when the farnesene concentration was as high as 1%.

It is important to note here that production yields can exceed tolerance levels. In these experiments, toxicity levels were measured using exogenous addition of the terpene at levels that inhibit growth, but production often continues long after growth stops,
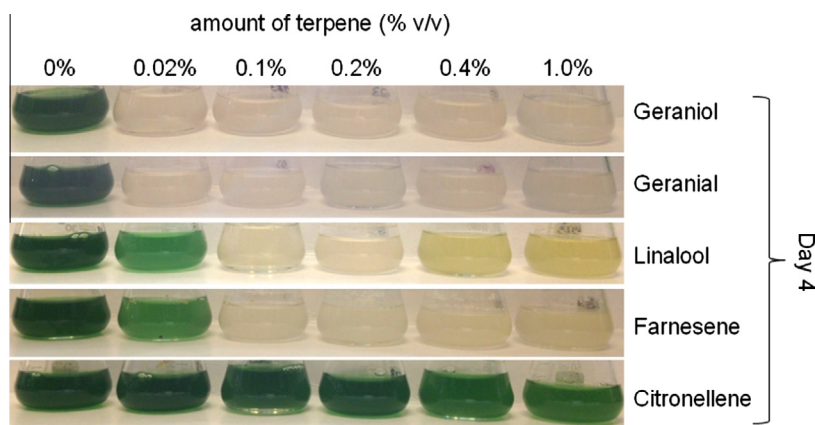

Fig. 25. Tolerance of *Synechocystis* to increasing amounts of the five compounds 4 days after addition.
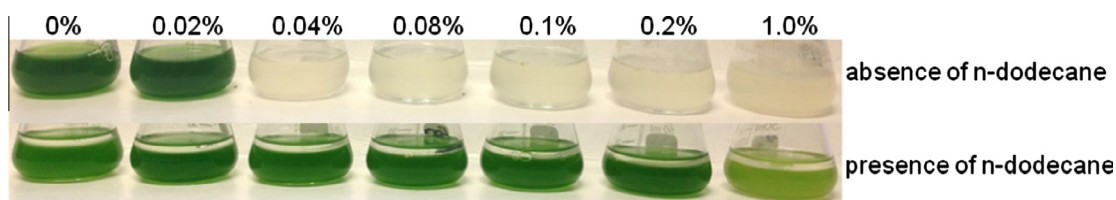

Fig. 26. Growth of *Synechocystis* in the presence of 0.1% v/v farnesene in the presence and absence of *n*-dodecane in the growth medium 4 days after addition.

allowing yields to exceed native tolerance levels [51]. Despite this, terpene toxicity still limits production and it will be essential to improve tolerance of selected microbial candidates in order to further increase yields.

4. Conclusions

1. Geraniol is a poor compression ignition fuel due to a long ignition delay. Of the changes that could be made to the molecular structure to improve the combustion and emission characteristics of the molecule, most beneficial was removal of a single H atom from the alcohol moiety of geraniol to form the aldehyde, geranial. Complete removal of the alcohol moiety and increasing the length of the alkenyl moiety, while maintaining a constant level of carbon branching and unsaturation, to form farnesene and squalene also results in a molecule of higher ignition quality.

2. Increasing the saturation of the alkenyl moiety of geraniol, and changing the configuration of a double bond in the alkyl moiety from *trans* to *cis*, suggested that the initial ignition delay of the terpenes when tested as single component fuels is dictated by the well understood low temperature reactions of alkyl and alkenyl radicals. However, a large influence of the various oxygenated functional groups of the terpenes on the reactivity of the alkenyl moiety was also apparent as the terpene that resembled solely the alkenyl moiety of geraniol, citronellene, exhibited the longest ignition delay of all the terpenes tested.

3. As single component fuels, the emissions characteristics of the terpenes are primarily driven by the duration of ignition delay and combustion phasing. However, in the case of squalene, a significantly higher viscosity than the other terpenes resulted in much larger emissions of particulate mass. This indicates an influence of fuel viscosity on the efficiency of fuel and air mixing via the fuel droplet size.

4. Blended with fossil diesel fuel, geranial and farnesene had no significant impact on combustion phasing up to a terpene content of 20%. At higher levels, the presence of either terpene resulted in a significantly longer duration of ignition delay and at a level of 60% terpene neither terpene and fossil diesel blend would combust. This suggests that the higher energy input experimental conditions employed in the tests of the terpenes as single fuel components activated low temperature radical branching routes not viable at the lower energy input experimental conditions employed when blending the geranial and farnesene with fossil diesel.

5. Geraniol was found not to be soluble with fossil gasoline. Citronellene and linalool, which were both found to be very poor diesel fuels, did however mix well gasoline and blends of up to 45% and 65% respectively were found to combust in a steady manner in a spark ignition engine.

6. The toxicity tests indicate that geraniol and geranial display a very toxic effect on cultures of *Synechocystis* even at low concentrations whilst linalool and farnesene are less toxic. Citronellene showed no evident toxic effect even at the highest concentration of 1% v/v, but unfortunately no citronellene synthesis enzyme has yet been identified in nature.

7. A two-phase system involving *n*-dodecane has been demonstrated to be a useful method of improving the survival of *Synechocystis* in the presence of farnesene.

References

[1] Peralta-Yahya PP, Zhang F, del Cardayre SB, Keasling JD. Microbial engineering for the production of advanced biofuels. Nature 2012;488(7411):320–8.
[2] Lu J, Sheahan C, Fu P. Metabolic engineering of algae for fourth generation biofuels production. Energy Environ Sci 2011;4(7):2451–66.
[3] Rude MA, Schirmer A. New microbial fuels: a biotech perspective. Curr Opin Microbiol 2009;12(3):274–81.
[4] Rosillo-Calle F, Walter A. Global market for bioethanol: historical trends and future prospects. Energy Sustain Dev 2006;10(1):20–32.
[5] Um BH, Kim YS. Review: a chance for Korea to advance algal-biodiesel technology. J Ind Eng Chem 2009;15(1):1–7.
[6] Demirbas A, Fatih Demirbas M. Importance of algae oil as a source of biodiesel. Energy Convers Manage 2011;52(1):163–70.
[7] Krohn BJ, McNeff CV, Yan B, Nowlan D. Production of algae-based biodiesel using the continuous catalytic Mcgyan-« process. Bioresour Technol 2011; 102(1):94–100.
[8] Yang J, Xu M, Zhang X, Hu Q, Sommerfeld M, Chen Y. Life-cycle analysis on biodiesel production from microalgae: water footprint and nutrients balance. Bioresour Technol 2011;102(1):159–65.
[9] Chisti Y. Biodiesel from microalgae. Biotechnol Adv 2007;25(3):294–306.
[10] Ahmad AL, Yasin NHM, Derek CJC, Lim JK. Microalgae as a sustainable energy source for biodiesel production: a review. Renew Sustain Energy Rev 2011; 15(1):584–93.
[11] Gallagher BJ. The economics of producing biodiesel from algae. Renew Energy 2011;36(1):158–62.
[12] Lee DH. Algal biodiesel economy and competition among bio-fuels. Bioresour Technol 2011;102(1):43–9.
[13] Campbell PK, Beer T, Batten D. Life cycle assessment of biodiesel production from microalgae in ponds. Bioresour Technol 2011;102(1):50–6.
[14] Delrue F, Setier PA, Sahut C, Cournac L, Roubaud A, Peltier G, et al. An economic, sustainability, and energetic model of biodiesel production from microalgae. Bioresour Technol 2012;111:191–200.
[15] Atsumi S, Higashide W, Liao JC. Direct photosynthetic recycling of carbon dioxide to isobutyraldehyde. Nat Biotechnol 2009;27(12):1177–80.
[16] Dunlop MJ, Dossani ZY, Szmidt HL, Chu HC, Lee TS, Keasling JD, et al. Engineering microbial biofuel tolerance and export using efflux pumps. Mol Syst Biol 2011;10:7.
[17] Ruffing AM. Engineered cyanobacteria: teaching an old bug new tricks. Bioengineered 2011;2(3):136–49.
[18] Ducat DC, Way JC, Silver PA. Engineering cyanobacteria to generate high-value products. Trends Biotechnol 2011;29(2):95–103.
[19] Vranova E, Coman D, Gruissem W. Structure and dynamics of the isoprenoid pathway network. Mol Plant 2012;5(2):318–33.
[20] Lindberg P, Park S, Melis A. Engineering a platform for photosynthetic isoprene production in cyanobacteria, using *Synechocystis* as the model organism. Metab Eng 2010;12(1):70–9.
[21] Reinsvold RE, Jinkerson RE, Radakovits R, Posewitz MC, Basu C. The production of the sesquiterpene beta-caryophyllene in a transgenic strain of the cyanobacterium *Synechocystis*. J Plant Physiol 2011;168(8):848–52.
[22] Hejazi MA, Holwerda E, Wijffels RH. Milking microalga *Dunaliella salina* for beta-carotene production in two-phase bioreactors. Biotechnol Bioeng 2004; 85(5):475–81.
[23] Tracy NI, Chen D, Crunkleton DW, Price GL. Hydrogenated monoterpenes as diesel fuel additives. Fuel 2009;88(11):2238–40.
[24] Peralta-Yahya PP, Ouellet M, Chan R, Mukhopadhyay A, Keasling JD, Lee TS. Identification and microbial production of a terpene-based advanced biofuel. Nat Commun 2011;2:483.
[25] Anand BP, Saravanan CG, Srinivasan CA. Performance and exhaust emission of turpentine oil powered direct injection diesel engine. Renew Energy 2010; 35(6):1179–84.
[26] Hellier P, Ladommatos N, Allan R, Payne M, Rogerson J. The impact of saturated and unsaturated fuel molecules on diesel combustion and exhaust emissions. SAE Int J Fuels Lubric 2011;5(1):106–22.
[27] Schönborn A, Ladommatos N, Williams J, Allan R, Rogerson J. Effects on diesel combustion of the molecular structure of potential synthetic bio-fuel molecules. SAE technical paper series, 2007-24-0125; 2007.
[28] Castenholz RW. Culturing methods for cyanobacteria. In: Lester Packer ANG, editor. Methods in enzymology cyanobacteria. Academic Press; 1988. p. 68–93.
[29] Westbrook CK. Chemical kinetics of hydrocarbon ignition in practical combustion systems. Proc Combus Inst 2000;28(2):1563–77.
[30] Salooja KC. Combustion studies of olefins and of their influence on hydrocarbon combustion processes. Combust Flame 1968 Oct;12(5):401–10.
[31] Murphy MJ, Taylor JD, McCormick RL. Compendium of experimental cetane number data. NREL/SR 540-36805 2004; September 1.
[32] Heyne JS, Boehman Aü L, Kirby S. Autoignition studies of *trans*- and *cis*-decalin in an ignition quality tester (IQT) and the development of a high thermal stability unifuel/single battlefield fuel. Energy Fuels 2009;23(12):5879–85.
[33] Hellier P, Ladommatos N, Allan R, Filip S, Rogerson J. The importance of double bond position and *cis trans* isomerisation in diesel combustion and emissions. Fuel 2013;105:477–89.
[34] Bounaceur R, Warth V, Sirjean B, Glaude PA, Fournet R, Battin-Leclerc F. Influence of the position of the double bond on the autoignition of linear alkenes at low temperature. Proc Combust Inst 2009;32(1):387–94.

[35] Schönborn A, Ladommatos N, Williams J, Allan R, Rogerson J. The influence of molecular structure of fatty acid monoalkyl esters on diesel combustion. Combust Flame 2009;156(7):1396–412.

[36] Mehl M, Pitz WJ, Westbrook CK, Yasunaga K, Conroy C, Curran HJ. Autoignition behavior of unsaturated hydrocarbons in the low and high temperature regions. Lawrence Livermore National Laboratory, Mail Stop L-367, 7000 East Avenue, Livermore, CA 94550, United States National University of Ireland, Galway, Ireland; 2011. p. 201–8.

[37] Salooja KC. The role of aldehydes in combustion: Studies of the combustion characteristics of aldehydes and of their influence on hydrocarbon combustion processes. Combust Flame 1965;9(4):373–82. Dec.

[38] Pilling MJ. Low-temperature combustion and autoignition. Elsevier; 1997.

[39] Ban-Weiss GA, Chen JY, Buchholz BA, Dibble RW. A numerical investigation into the anomalous slight NOx increase when burning biodiesel; a new (old) theory. Fuel Process Technol 2007;88(7):659–67.

[40] Szybist JP, Boehman AL, Taylor JD, McCormick RL. Evaluation of formulation strategies to eliminate the biodiesel NOx effect. Fuel Process Technol 2005;86(10):1109–26.

[41] Mueller CJ, Boehman AL, Martin GC. An experimental investigation of the origin of increased NOx emissions when fueling a heavy-duty compression-ignition engine with soy biodiesel. SAE technical paper series 2009-01-1792; 2009.

[42] Tree DR, Svensson KI. Soot processes in compression ignition engines. Prog Energy Combust Sci 2007;33(3):272–309.

[43] Ladommatos N, Rubenstein P, Bennett P. Some effects of molecular structure of single hydrocarbons on sooting tendency. Fuel 1996;75(2):114–24.

[44] Park SH, Youn IM, Lee CS. Influence of ethanol blends on the combustion performance and exhaust emission characteristics of a four-cylinder diesel engine at various engine loads and injection timings. Fuel 2011;90(2):748–55.

[45] Pidol L, Lecointe B, Starck L, Jeuland N. Ethanol–biodiesel–diesel fuel blends: performances and emissions in conventional diesel and advanced low temperature combustions. Fuel 2012;93:329–38.

[46] Andogan B, Baydar H, Kaya S, Demirci M, Ozbasar D, Mumcu E. Antimicrobial activity and chemical composition of some essential oils. Arch Pharm Res 2002;25(6):860–4.

[47] Azevedo MMB, Pereira AQ, Chaves FCM, Bizzo HR, Alviano CS, Alviano DS. Antimicrobial activity of the essential oils from the leaves of two morphotypes of *Croton cajucara* Benth. J Essential Oil Res 2012;24(4):351–7.

[48] Onawunmi GO. Evaluation of the antimicrobial activity of citral. Lett Appl Microbiol 1989;9(3):105–8.

[49] Sato K, Krist S, Buchbauer G. Antimicrobial effect of vapours of geraniol, (R)-(−)-linalool, terpineol, Y-terpinene and 1,8-cineole on airborne microbes using an airwasher. Flavour Fragr J 2007;22(5):435–7.

[50] Somolinos M, Garcia D, Condon S, Mackey B, Pagan R. Inactivation of *Escherichia coli* by citral. J Appl Microbiol 2010;108(6):1928–39.

[51] Dunlop M. Engineering microbes for tolerance to next-generation biofuels. Biotechnol Biofuels 2011;4(1):32.